AFRL-SN-RS-TR-2004-315
Final Technical Report
November 2004

INVESTIGATION OF RADIATION RESISTANT MATERIALS FOR DEVELOPING SPACE-HARDENED POLYMER MODULATORS

International Photonics Consultants, Inc.

APPROVED FOR PUBLIC RELEASE; DISTRIBUTION UNLIMITED.

AIR FORCE RESEARCH LABORATORY
SENSORS DIRECTORATE
ROME RESEARCH SITE
ROME, NEW YORK

STINFO FINAL REPORT

This report has been reviewed by the Air Force Research Laboratory, Information Directorate, Public Affairs Office (IFOIPA) and is releasable to the National Technical Information Service (NTIS). At NTIS it will be releasable to the general public, including foreign nations.

AFRL-SN-RS-TR-2004-315 has been reviewed and is approved for publication

APPROVED: /s/
JAMES E. NICHTER
Project Engineer

FOR THE DIRECTOR: /s/
GERALD J. GENELLO
Acting Chief, Rome Operations Office
Sensors Directorate

REPORT DOCUMENTATION PAGE

Form Approved
OMB No. 074-0188

1. AGENCY USE ONLY (Leave blank)	2. REPORT DATE	3. REPORT TYPE AND DATES COVERED
	November 2004	**FINAL** **Jul 02 – May 04**

4. TITLE AND SUBTITLE

INVESTIGATION OF RADIATION RESISTANT MATERIALS FOR DEVELOPING SPACE-HARDENED POLYMER MODULATORS

5. FUNDING NUMBERS

C - F30602-02-C-0157
PE - 62204F
PR - 665D
TA - SN
WU - 03

6. AUTHOR(S)

Edward W. Taylor

7. PERFORMING ORGANIZATION NAME(S) AND ADDRESS(ES)

International Photonics Consultants, Inc.
30 Tierra Monte NE
Albuquerque NM 87122

8. PERFORMING ORGANIZATION REPORT NUMBER

N/A

9. SPONSORING / MONITORING AGENCY NAME(S) AND ADDRESS(ES)

AFRL/SNDP
26 Electronic Parkway
Rome NY 13441-4514

10. SPONSORING / MONITORING AGENCY REPORT NUMBER

AFRL-SN-RS-TR-2004-315

11. SUPPLEMENTARY NOTES

AFRL Project Engineer: James E. Nichter/SNDP (315) 330-7423 James.Nichter@rl.af.mil

12a. DISTRIBUTION / AVAILABILITY STATEMENT

APPROVED FOR PUBLIC RELEASE; DISTRIBUTION UNLIMITED.

12b. DISTRIBUTION CODE

13. ABSTRACT ***(Maximum 200 Words)***

An investigation of the radiation resistance of polymer based electro-optic modulators was conducted by the International Photonics Consultants for the Air Force Research Laboratory Photonics Technology Branch (SNDP) to determine the potential of polymer modulators for airborne and space environment microwave applications. Gamma-ray and proton irradiation of CPW-1/APC, CLD-75/APC, and other non-linear polymer materials received ionizing doses ranging to 163 krad(Si). Modulator parameters including half-wave voltage, insertion losses, and extinction ratios were evaluated for changes resulting from the ionization processes. Among the different spun-on and self-assembled PBMs investigated CPW-1/APC phenyltetraene based devices exhibited the greatest resistance to both gamma-ray and proton irradiations. In some devices the half-wave voltage and insertion losses decreased at low [50 krad(si)] gamma-ray total dose. Empirical data supporting a recent hypothesis was demonstrated which asserted that strongly poled PBMs exhibiting low V_π are less susceptible to moderate gamma-ray dose. Compared to gamma-ray irradiations, PBMs exposed to 25.6 MeV energetic protons at equivalent dose were shown to exhibit increased degradation to their V_π and insertion losses. The empirical data provide a critical step in addressing DoD concerns for developing radiation resistant polymer technology for application to next generation microwave integrated polymer photonic components for space and strategic systems.

14. SUBJECT TERMS

irradiation, polymer, radiation resistance, modulator, photonic

15. NUMBER OF PAGES 71

16. PRICE CODE

17. SECURITY CLASSIFICATION OF REPORT	18. SECURITY CLASSIFICATION OF THIS PAGE	19. SECURITY CLASSIFICATION OF ABSTRACT	20. LIMITATION OF ABSTRACT
UNCLASSIFIED	UNCLASSIFIED	UNCLASSIFIED	UL

TABLE OF CONTENTS

LIST OF FIGURES

LIST OF TABLES

SUMMARY

An investigation of the radiation resistance of polymer based electro-optic modulators was conducted by the International Photonics Consultants, Inc., for the Air Force Research Laboratory Photonics Technology Branch (SNDP). Passive gamma-ray and proton irradiation of state-of-the–art and emerging polymer based modulators (PBMs) and materials provided by AFRL organizations and commercial sources were investigated to determine their potential for airborne and space environment microwave applications. PBMs with active core regions composed of CPW-1/APC, CLD-75/APC, LD3, PCBS and other electro-optic linear and non-linear materials were irradiated to ionizing doses ranging to ~163 krad(Si). Key modulator operational parameters including half-wave voltage, propagation losses, and extinction ratios were evaluated for changes resulting from the ionization process. Among the different spun-on and self-assembled PBMs studied, CPW-1/APC and CLD-75/APC based devices exhibited the greatest resistance to both gamma-rays and proton irradiations. In some CPW-1/APC and CLD-75/APC devices both the half-wave voltage and insertion losses were observed to decrease at low [~10-163 krad(Si)] gamma-ray total dose. Empirical data in support of a recent hypothesis asserting that strongly poled PBMs exhibiting low half-wave voltages are less susceptible to moderate gamma-ray dose was demonstrated. Preliminary data indicates that the mechanism for this behavior is linked to the increased free volume generated in the modulator materials as a result of predominantly cross-linking processes. Compared to gamma-ray irradiation results, modulators exposed to 25.6 MeV energetic protons at equivalent dose were shown to exhibit increased degradation in V_π and increased insertion losses. These empirical results provide a first but critical step in addressing DOD concerns for developing radiation resistant polymer technology suitable for rapid development of next generation microwave integrated polymer photonic components for space and strategic system applications.

INTRODUCTION

The expected near-term emergence of economical high speed, large bandwidth polymer based photonic (PBP) devices has drawn attention to ascertaining the potential performance of specific components such as polymer modulators, waveguides and photodetectors in space and strategic radiation environments. While there have been various claims that many polymer materials used in fabricating PBPs are intrinsically resistant to ionizing radiation, verification to this extent has only been recently investigated [1-12]. Recent studies clearly indicate that to favorably and efficiently impact the development of cutting-edge organic/polymer based photonics technology for reliable operation in the space-radiation environment, acquisition of empirical irradiation data and a thorough analysis of the radiation induced effects are required at the earliest stages of component development. Often device and system radiation resistance studies are ignored or postponed until a fully mature technology is in-hand, requiring initiation of expensive hardening investigations which result in abandoning, redesign or extensive modification of the developed technology. The latter two practices inevitably lead to using radiation-shielding or elaborate device upset circumvention practices, which add to the volume, weight, cost and complexity of the application.

The following objectives were successfully completed under this investigation:

- Fabricate, Characterize and Irradiate ESA and other State-of–the–Art Polymer EO Modulators and Materials
- Analyze and Determine Resistance of Modulators to Ionizing Space Radiation Environments
- Provide Empirical Data Base for Advancing the Development of Hardened Microwave Modulator Technologies
- Advance AFRL/SNDP R & D of Hardened Next-Generation Space & Missile Technology and Applications

To date, knowledge and published data regarding the radiation resistance of EO polymer modulators and associated components grown by specific polymer processing techniques (e.g. ESA, spin on, epitaxial lift off, reactive ion etching, etc.) is virtually nonexistent, and largely consists of specific investigations reported or being investigated by the International Photonics Consultants (IPC) for commercial, DOD agencies and AFRL organizations (AFRL/SNDP, AFRL/VSSS and AFRL MLPSO). As such, the data base for radiation induced effects in leading polymer photonic technologies is beginning to emerge.

Very recent experimental results have been reported by IPC staff and their colleagues regarding the induced effects of ionizing radiation on a limited sample size of select poled and non-poled polymer materials for potential application to large bandwidth and high speed polymer EO modulators and emerging polymer photodetectors [1-4, 9-11]. Empirical data resulting from these studies indicated a very high potential for developing radiation resistant, stable, high bandwidth and efficient polymer based EO modulators and associated components such as polymer photodetectors that can survive in space radiation environments and potentially survive in high dose strategic environments.

For this investigation, an impressive variety of polymer modulators and materials were provided by AFRL/SNDP, AFRL/MLPSO, Pacific Wave Industries (PWI), IPITEK and Nanosonic Inc.(NS) for the irradiation investigations. These devices were varied in their compositions representing in most cases a small sample set of state-of-the-art and emerging linear and nonlinear optic (NLO) electro-optic (EO) polymer materials including guest –host materials. Emphasis was placed on investigating phenyltetraene bridged chromophores with amorphous polycarbonate (CPW-1/APC), CLD-75/APC and a second guest-host system LD3, which was composed of PMMA containing 4-[bis(2-hydroxyethl)amino]-4'-[(methylacryloyl-hxyl)sufonyl] azobenzene chromophores [13,14]. Other polymer modulator materials and devices included salmon DNA [HexadeCetylTriMethylAmmonium Chloride (CTMA)] NLO films and a hybrid polymer modulator composed of an electrostatic self-assembled (ESA) thin film consisting of PCBS {Poly{1-[4-(3-carboxy-4-hydroxyphenylazo)benzene-sulfonamido]-1,2-ethanediyl

sodium salt} combined with spun-on NLO materials. The wide array of modulators differing in composition provided a diverse look at potentially radiation resistant PBMs.

The CPW-1/APC and CLD-75/APC devices exhibited the greatest resistance to both gamma-rays and proton irradiations. In some devices both the half-wave voltage and insertion losses were observed to decrease at low [~50 krad(Si)] gamma-ray total dose while proton irradiation was observed to cause greater degradation. In either case the radiation induced changes in the CPW-1/APC and CLD-75/APC devices showed excellent resistance to proton and gamma-rays irradiation to the total dose applied.

Empirical data in support of a recent hypothesis asserting that strongly poled PBMs exhibiting low half-wave voltages are less susceptible to moderate gamma-ray dose was also demonstrated as collaborated by the SNDP and PWI device response data.

As reported herein, the results provided convincing data that the potential for realizing highly radiation resistant polymer modulators is excellent and should result in hardened devices as the processing, poling and stability of the devices with regards to environmental factors improves.

IRRADIATION OF PBMS BY GAMMA-RAYS: DATA AND RESULTS

Gamma-ray irradiation of PBMs was conducted using the Gamma-Ray Irradiation Facility (GIF) located at the Sandia National Laboratory (SNL) in Albuquerque, NM. Shown in Figure 1 is the setup under which the gamma-ray irradiations of the device samples were conducted. Thermoluminescent detector (TLD) arrays for measuring

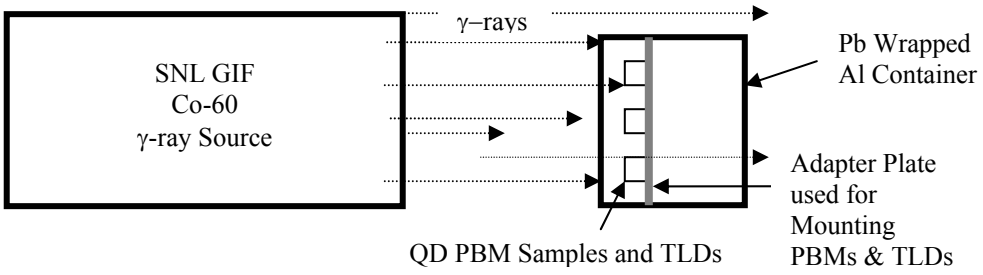

Figure 1. Gamma-ray irradiation of PBM samples. A lead (Pb) wrapped aluminum (Al) container (Pb-Al) was used to reduce low energy photon spectrum and to shield the samples from ambient photo-degradation effects. PPDs and TLDs for measuring the gamma-ray dose were located in proximity to each other. Direction of gamma-rays (γ-rays) are shown by arrows.

the gamma-ray dose were mounted on an acrylic adapter plate in proximity to each PBM. As can be seen in Figures 1 and 2 the modulator samples were oriented perpendicular to the gamma-ray source.

Figure 2a shows the orientation of the Pb-Al container (irradiation volume) which housed the PBM devices during irradiation, while Figure 1b illustrates a typical stacked array of two Pb-Al irradiation volumes under irradiation by gamma-rays. The SNL dosimetry was optimized using a Pb-Al container (also referred to as the irradiation volume) to attenuate the low energy photons since the presence of these photons in the incident spectrum can cause dosimetry errors [15]. This assured that lower energy photons (< 1 MeV) were greatly attenuated or absorbed in the Pb-Al container walls. Low energy photons are created by Compton scattering of the Co-60 gamma-rays within the source structure or within materials that lay between the source and the irradiated device, as well as within materials that lie beyond the device but contribute to backscattering. The container also

prevented unwanted exposure of the samples to sustained periods of room lighting which is known to induce "aging" in the PBM samples via photo-degradation processes. The uncertainty in the SNL-GIF dosimetry measurements was ~10%.

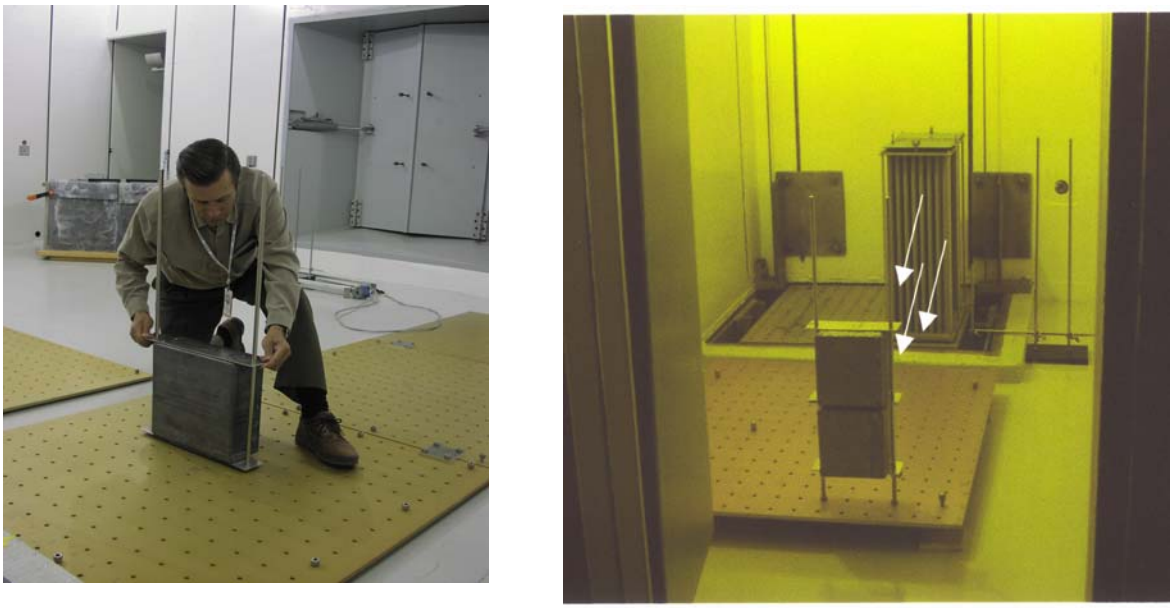

(a) (b)

Figure 2. Sandia National Laborratory Gamma-ray Irradiation Facility. Set-up (a) for typical SNL-GIF passive irradiation of polymer modulator devices. The arrows in (b) indicate the direction of gamma-rays from the raised gamma-ray source.

Prior to the onset of irradiation, gamma-ray dose and dose rate mapping was accomplished to ascertain dose rate variations and to identify the optimum spatial coordinates required for aligning the samples perpendicular to the gamma-ray source. Following incremental irradiations, selected samples were removed from the acrylic holder plate and placed in a light–tight protective storage container occupied by the control sample. Dosimetry considerations consisted of selecting the proper number and type of dosimeters for confidently measuring the irradiation dose, and locating the dosimeters in proximity to the samples. Multiple CaF_2 TLD arrays consisting of 4 TLDs per array measured the dose received by each sample. The array arrangement insured an accurate measurement of the gamma-ray dose received by each sample and provided multiple dose point readings for averaging the total dose across the target area. The irradiated TLD arrays were removed following each incremental irradiation and replaced by fresh TLDs in readiness for the next incremental irradiation.

The glow-curve readings of the TLDs and the dose and dose rate statistics were performed by the SNL Radiation Metrology Laboratory. The standard deviation in dose are SNL estimates based on random uncertainties in TLD responses at Co-60 energies and are reported at the 1-sigma level. At Co-60 energies, the Dose (Si) is calculated as Dose (Si) = Dose (CaF_2) x 1.02.

RESPONSES OF IRRADIATED AFRL/SNDP PBMS

Gamma-ray irradiations were performed on three sample sets of AFRL/SNDP PBM devices and modulator materials fabricated to operate at a wavelength λ = 1550 nm as shown in Table 1. Figure 3 is a representation of the design, composition and cross section of the three sample sets of irradiated modulators. Shown are cross sections of

Table 1. Gamma-ray irradiation parameters.

SNDP Sample Set	No. of Irradiated PBM Samples	Poling Conditions Maximum [Temp. (ºC) / Voltage (V)]	Dose Range [D_γ, [krad(Si)] (10%)	Dose Rate $D_\gamma(t)$, [rad (Si) sec^{-1}] (10%)
1.	5	150 / 500	10.0 - 104	1.74
2.	5	150 / 450	10-100	1.94
3.	6	160 / 450	163	2.10

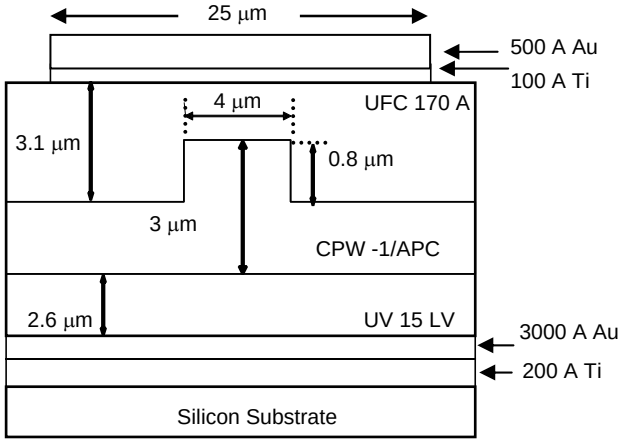

Figure 3. AFRL/SNDP CPW-1/APC (CLD-1) MZ modulator cross-section.

the modulator core, clad and electrode regions as well as the ridge waveguide design of the active core region composed of the ring-locked phenyltetraene-based second order NLO chromophore CPW-1/APC also referred to as CLD-1/APC.

The device design, its structure and processing of the chromophoric core, application of the conductive cladding materials and the assembly of the modulator emulated the techniques and approach described by Zhang and Dalton for APC/CLD-1 modulators [14]. For a 25 wt % CLD-1 core, Zhang and Dalton and colleagues reported modulators exhibiting strong photochemical stability at ~ 45-50 ºC, an optical loss of 1.7 dB/cm, average EO coefficients of 92 pm/V in corona poled films, a modulation voltage of 3.7 V and an extinction ratio of 26 dB at 1.55 μm. The AFRL/SNDP modulator was composed of a mixture of amorphous polycarbonate (APC) with a 25 % loading of CPW-1. This mixture was prepared by making a 12% solid weight to solvent ratio in trichloroethane and spin casting it on to the lower cladding to yield a 3 μm core thickness. The solvent was dried out by placing the sample first onto a hot plate and then into an oven at 125 C. Ridge waveguides were formed by RIE etching. The upper cladding was composed of a UV curable material (UFC 170 A, Uray Corp., Korea) and following spin casting was UV and heat treated. Thickness of this cladding layer was 3.1 μm, while the total device thickness was 7.9 μm. Poling of the device was accomplished using metal electrodes on top of the upper cladding and also served as the driving electrode. The composition of the electrode was 100 A Ti and 500 A of Au. The width of the electrodes (microstrip lines) was 40 μm and was not optimized to achieve 50 Ohm characteristic impedance. Poling fields applied over the devices were varied from 400-750 V for 15-28 minutes while the maximum temperature was varied to 140, 150 and 160 ºC for different devices. In this manner, chromophores were frozen into the polymer matrix by removing the heat while the poling voltage was still applied.

As shown in Table 1, the first set of CPW-1/APC devices were irradiated at an average dose rate of 1.74 rad(Si)·sec^{-1}. The dose rates shown in Table 1 are somewhat elevated above the very low dose rates that can be experienced by satellites in some near Earth–orbits, and were chosen to satisfy economic and time-constraints for conducting the

study. However, the rates were well within the usual dose rate ranges used by other investigators concerned with examining the effects of the ionizing space environment on photonic, optoelectronic and electro-optic systems and components. In essence, the irradiated samples and devices exhibited response behavior under accelerated dose rate/dose conditions, thereby providing an upper bound to potentially induced damage phenomena within the NLO materials and EO devices.

Figure 4a depicts the measurement apparatus used by SNDP in measuring modulator half-wave pre- and post- irradiation waveform voltages, while Figure 4(b) is a typical oscilloscope trace of the post–irradiation V_π response of modulator samples.

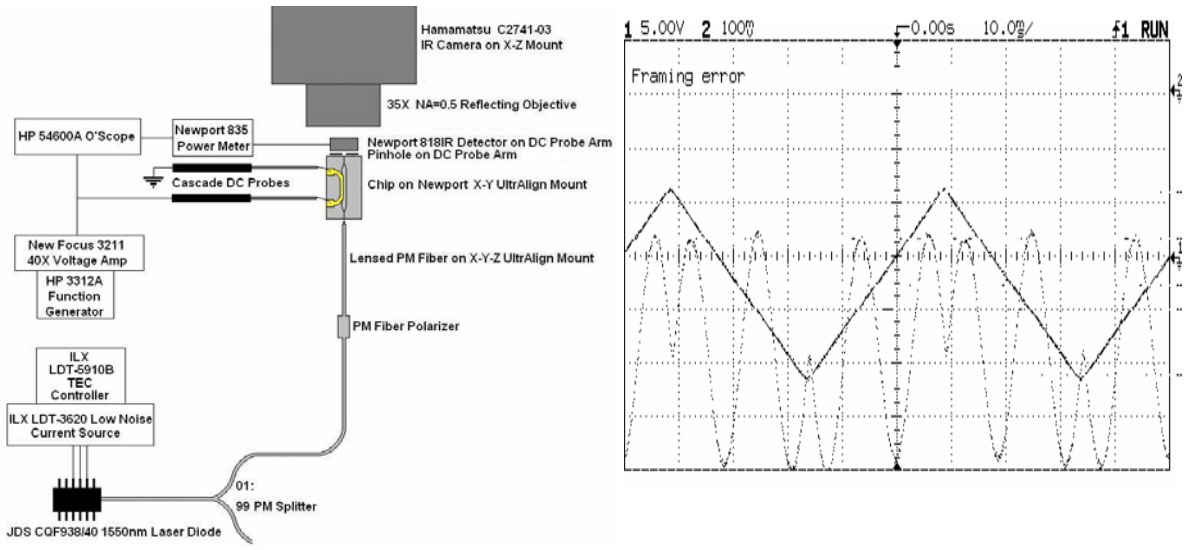

(a) (b)

Figure 4. SNDP apparatus for measuring modulator voltage waveforms. Shown in (a) is the technique for injection of 2 mW polarized light into the modulator device and (b) shows a modulated waveform [1].

The voltage required to induce a π-phase change (100 % modulation) is referred to as the half wave voltage (V_π) and, under ideal conditions is inversely related to the polymer material EO coefficient (i.e. r_{33}) given by the expression:

$$V_\pi = \lambda\, d\, /(n^3\, r_{33}\, \Gamma\, L) \qquad (1)$$

Here λ is the modulator operational wavelength; (Γ) represents a quality factor that measures the overlap between the electric and optical fields and device geometry (Γ = 1 for large electrode devices and < 1 for high speed impedance– matched devices); L represents the interaction length of the electrodes over the modulator waveguides; and the distance between the electrodes and the active core region is represented by "d". These parameters can be shown to be nearly invariant under the applied low-dose [~ 100 krad(Si)] gamma-irradiation, however, the behavior of the refractive index of the modulator active core (n) and claddings under irradiation conditions was not directly measured and caution must be exercised in interpreting the post-irradiation results.

As shown in Table 2 and 3, PBM Sample Set 1 varied widely in pre- and post-irradiation response data. V_π values ranged by an order of magnitude in the pre-irradiation measurements of the six samples. Of the six samples poled, sample 2 (R1D2) provided indications of having received the strongest poling (see Appendix1, Poling Profile 5) which is evidenced by its low V_π value of V_π = 4.4 V. This sample also displayed very consistent performance in other modulator parameters such as having a low insertion loss (IL = 2.7 dB/cm) and the highest pre-irradiation measured values for optical modulation depth (OMD = 92 %) and an extinction ratio of ER = 14 dB.

Table 2. Pre- and post irradiation responses of SNDP PBMs (Sample Set 1).

Sample Set 1	Dose [krad(Si)]	V_π Pre-Irrad) (V)	V_π Post-Irrad (V)	ΔV_π (%)	IL* Pre-Irrad (dB/cm)	IL* Post-Irrad (dB/cm)	ΔIL (dB/cm)
1. R3D2	104	44	48	9.1	5.6	2.2	-3.4
2. R1D2	100	4.4	4.4	0	2.7	2.1	-0.6
3.R3D3	49.2	7.7	6.9	-10.4	6	2.4	-3.6
4. R17D1	49.2	27.6	28	1.4	2.4	3.4	1.0
5. R3D1	10	41	not measurable	N/A	not measured	5.8	N/A
6. R5D2 Control	0	29.3	27	-7.8	not measured	2.7	N/A

***Note 1: 6 dB coupling loss included,**

Table 3. Pre- and post-irradiation responses of SNDP PBMs (continued).

Sample Set 1 (cont'd)	Dose [krad(Si)]	OMD** Pre-Irrad (%)	OMD** Post-Irrad (%)	ΔOMD (%)	ER** Pre-Irrad (dB)	ER** Post-Irrad (dB)	ΔER (dB)
1. R3D2	104	55	90	45	5	13	8
2. R1D2	100	92	47	-45	14	4.5	-9.5
3. R3D3	49.2	61	56	-6.0	6	5.6	-0.4
4. R17D1	49.2	78	94	16	9	15	6
5. R3D1	10	31	not measurable	N/A	3	not measurable	N/A
6. R5D2 Control	0	19	79	60	2	9.3	7.3

****Note 2: accuracy in these measurements is considered to be +/- 7 dB.**

The most consistent pre- and post- irradiation results for determining the influence of ionizing radiation on the modulator half-wave voltages were exemplified by the behavior of samples 1-4 in Tables 2 and 3. The data suggest that well-poled modulators with low V_π are potentially stable in the presence of the gamma-ray doses used in this study [$D_\gamma \leq$ 100 krad(Si)]. This assumption can be argued by considering the behavior of sample 2 irradiated at D_γ = 100 krad(Si). Following the irradiation, no observable change was observed in its half wave voltage ($\Delta V_\pi = 0$). Using Eq. 2, r_{33} for sample 2 is calculated to be r_{33} = 57 pm/V assuming that the overlap interval $\Gamma = 1$. SNDP accuracy in measuring V_π was repeatable at +/- 3%. However, samples 1 and 4 possessing large V_π values of 44V and 27.6 V, respectively, showed noticeable increases in V_π following irradiation.

In contrast to samples 1, 2 and 4, the post-irradiation measurement of sample 3 showed a very large decrease in V_π (ΔV_π = -10.4 %). Like sample 3, the post-irradiation measurement of the control sample 6 also exhibited a decrease from its initial (pre-irradiation) V_π value. Sample 5 was irradiated at D_γ = 10 krad(Si) but due to its instability, and signal drift, measurement of its V_π prior to irradiation was not accomplished. These widely varying preliminary results suggest that modulator devices not strongly poled are likely to be unstable and perhaps also affected more by a moderate

ionizing radiation dose [i.e. ~50 - 104 krad(Si)] than strongly poled devices. Consideration must also be given to the premise that instabilities of the weakly poled devices may have masked the extent of radiation induced effects shown in Tables 2 and 3.

Ionizing radiation induced damage is strongly suggested in the observed response of sample 1, and to a lesser extent in sample 4. These devices were irradiated at doses of D_γ = 104 krad(Si) and D_γ = 49.2 krad(Si), respectively and their increases in V_π appears to scale with dose and display behavior opposite that of the non-irradiated control sample. It is possible that the ΔV_π behavior exhibited by these two devices resulted from ionization induced changes to the CPW-1 dipole moments thereby reducing the magnitude of r_{33}. However, the specific contribution of radiation induced de-poling in regards and relative to other known environmental and atmospheric de-poling processes (e.g. temperature, humidity, photochemical, etc.) is largely unknown and is necessary in order to resolve these interesting and empirical issues.

As shown in Table 2, following irradiation, samples 1 and 3 experienced large reductions to their pre-irradiated insertion loss measurements (ΔIL = -3.4 to -3.6 dB/cm). The large pre-irradiation insertion loss measurements may be indicative of imperfections and defects in the waveguide regions, perhaps resulting from the reactive ion etching (RIE) processing. The presence of unwanted impurities and traps within the devices must also be considered. In contrast, low pre-irradiation IL values were exhibited by samples 2 and 4 (IL = 2.7 dB/cm and 2.4 dB/cm, respectively) indicating well–fabricated waveguides. As shown in Table 2, sample 2 exhibited the least response to the gamma-ray irradiations (ΔIL = -0.6 db/cm) while sample 4 changed by ΔIL = 1 dB/cm. Following irradiation, the insertion loss of samples 1-3 were reduced from an average pre-irradiated value of 4.8 dB/cm to an average post–irradiated value of 2.2 dB/cm indicating that perhaps a measure of radiation induced filling of traps by free carriers may have occurred thereby reducing scattering and absorption centers in the active waveguide, cladding and cladding-core interface regions. One possible result of this interaction would be improved coupling of light to the guiding layer due to alteration the refractive indices in the core to

determine the exact mechanism(s) responsible for the reduction in the losses. Among the samples irradiated, sample 2 again exhibited excellent stability in the presence of ionizing radiation. The uncertainty in the IL measurements was ~ 2 dB/cm and the results must be viewed with some caution.

Table 3 shows wide variances in the OMD and ER pre- and post-irradiation measurements performed by SNDP. These interrelated measurements provide an estimate of the dynamic range of the modulator by examination of the signal intensities exiting the modulator device. The OMD for the samples were determined from the modulator responses using voltage waveform response data as shown in Figure 4. A determination of the MZ ER can be calculated via the relationship ER = V_{max} / V_{min} (dB), while the OMD is calculated from the extinction ratio by the relationship

$$OMD = (ER - 1) / (ER + 1) \times 100\% \qquad (2)$$

OMD values above 90% are considered to be indicative of good modulator performance and as may be observed in Table 3, sample 2 exhibited the largest extinction ratio (14 dB) and optical modulation depth (92 %), both measured prior to irradiation. Both samples 1 and 2 exhibited decreases to their ER and OMD values following irradiation. At a dose D_γ = 100 krad(Si) sample 2 displayed the lowest post-irradiation extinction ratio (4.5 dB) and lowest optical modulation depth (47 %). Samples 1 and 4 which possessed among the largest V_π values of V_π = 44 V and 27.6 V, respectively, also had the highest and lowest insertion losses (IL = 5.6 dB/cm and 2.4 dB/cm, respectively) and were observed to have the best post-irradiated ER and OMD responses.

Following irradiation of sample 1 to D_γ = 104 krad(Si), V_π was observed to increase by 9.1 %, and the extinction ratio increased by 8 dB while the OMD increased by 45 %. These are significant and desirable changes in ER and OMD but do not necessarily reflect an overall improvement in the modulator performance since V_π was increased. What is equally interesting is that the ER and OMD for samples 2 and 3 both possessing low V_π values, were apparently adversely affected by the gamma-rays. One possible explanation

for these contrasting results is that large measurement inaccuracies may have resulted during the ER and OMD measurements due to various factors such as establishing good electrode grounding, necessary for accurately measuring V_{max} and V_{min} (see Figure 4). Potential measurement errors ranging to 7 dB could have been responsible for the mixed ER and OMD results.

The data provided for the non-irradiated modulator control sample shown in Tables 2 and 3 also provides additional insight into the stability and behavior of the irradiated samples. The control sample was located in proximity to the irradiation area, not irradiated, but was exposed to approximately the same room temperature conditions as the irradiated samples. All samples were typically exposed to ambient (very low) room lighting during set up (approximately 25 minutes exposure time, each) prior to the irradiations and later during removal from the irradiation chamber for a period of approximately 12 minutes (each) to room-light. The V_{π} pre- and post irradiation measurements on all samples were conducted at AFRL/SNDP within approximately 72-96 hours following cessation of all irradiations. It would appear that the control sample improved in its V_{π}, OMD and ER values over a period of several weeks between the pre- and post-irradiation studies.

This behavior is contrary to that expected or reported for most NLO EO polymer thin film devices [7, 8, 10, 11, 14]. Previous studies have shown that operation of similar CLD-1 devices under inert gas environments have remained stable in operation while CLD-1 devices operated under normal atmospheric conditions deteriorate with time [14].

The control sample behavior is an indication that perhaps, with the exception of sample 2, significant material instabilities were present in the samples. As such, the determination of the exact role that environmental and ionizing radiation has in degrading the various modulator parameters is complex and beyond the scope of this effort.

Shown in Tables 4 and 5 are the pre-and post- irradiation responses for Sample Sets 2 and 3, respectively.

Table 4. Pre- and post- irradiation responses of SNDP PBMs (Sample Set 2)

Sample Set 2* & **(Sample No.)**	**V_π** (V)	**ER** (dB)	**6μm Straight WG Losses (dB)**		**4 μm Straight WG Losses (dB)**		**2 cm V_π push-pull equivalent (V)**	**Dose** [krad(Si)]
1. Jul03R6D2								10
Pre-Irrad.	8.8	12.4	7.6	6.2	8.1	4-3	4.30	
Pre- Irrad.	9.2	12.8	7.6	6-2	8.0	4-3	4.60	
Post- Irrad.	9.2	10	7.8	6-2	8.2	4-3	4.60	
2. Jul03R7D1								**Control**
Pre- Irrad.	12.0	12.3	7.5	6-1	8.1	4-2	3.00	
Pre- Irrad.	11.6	10.2	7.1	6-1	8.0	4-2	2.90	
Post- Irrad	12.0	14.7	7.1	6-1	7.9	4-2	3.00	
3. Jul03UV7D2								100
Pre- Irrad.	8.7	15.2	9.3	6-2	10.6	4-3	4.35	
Pre- Irrad.	9.2	8.5	9.6	6-2	10.8	4-3	4.60	
Post- Irrad.	9.0	17.1	10.3	6-2	#		4.50	
4. Jul03UV7D3								50
Pre-Irrad.	4.9	12.3	9.3	6-1	9.5	4-4	2.45	
Pre- Irrad.	5.2	10.6	10.1	6-1	9.8	4-4	2.60	
Post- Irrad.	5.2	12.8	Device cracked in two places					
5. Jul03UV9D1								50
Pre- Irrad.	9.8	14.6	8.2	6-3	9.4	4-1	2.45	
Pre- Irrad.	9.6	10.2	7.9	6-3	9.0	4-1	2.40	
Post- Irrad.	10.2	17.9	7.8	6-3	8.7	4-1	2.55	
6. Jul03UV9D3								100
Pre- Irrad.	4.7	11.1	7.8	6-3	9.2	4-2	2.35	
Pre- Irrad.	4.9	13.3	7.9	6-3	9.6	4-2	2.45	
Post- Irrad.	5.0	7.2	8.1	6-3	9.3	4-2	2.50	
7. Jul03UV13D2								10
Pre- Irrad.	5.6	13.9	10.4	6-1	NM	4-2	2.80	
Pre- Irrad.	5.8	10.6	10.3	6-1	12.2	4-2	2.90	
Post- irrad.	5.8	11.4	10.8	6-1	12.3	4-2	2.90	

*Note: Chips were processed by using protiated methanol (CH3OH).

Table 5. Pre- and post- irradiation responses of SNDP PBMs (Sample Set 3).

SNDP Sample Set 3* **(Sample No.)**	**V_π (V)**	**ER (dB)**	**6μm Straight WG Losses (dB)**		**4 μm Straight WG Losses (dB)**		**2 cm V_π Push-Pull Equivalent (V)**	**Dose [krad(Si)]**
1. Dec03R4D1								163
Pre- Irrad.	12.4	11.35	7.6	6-2	8.4	4-2	3.10	
Post- Irrad.	12	15.7	8.6	6-2	8.9	4-2	3.00	
2. Dec03R10D2								163
Pre- Irrad.	8.4	13.0	8.2	6-3	8.8	4-2	4.20	
Post- Irrad.	NM	NM	NM	NM	NM	NM	NM	
3. Dec03 R7D1								163
Pre- Irrad.	10.6	14.3	7.0	6-3	7.9	4-1	2.65	
Post- Irrad.	9.2	18.9	7.6	6-3	8.3	4-1	2.30	
4. Dec03R6D3								**Control**
Pre- Irrad.	5.6	10.0	10.5	6-1	NM		2.80	
Post- Irrad.	5.2	16.3	9.9	6-1			2.60	
5. Dec03R6D2								163
Pre- Irrad.	5.0	11.5	8.7	6-4	9.5	4-4	2.50	
Post- Irrad.	NM	NM	NM	NM	NM	NM	NM	
6. Dec03R9D3								163
Pre- Irrad.	5.4	20.0	9.4	6-3	9.3	4-2	2.70	
Post- Irrad.	NM	NM	NM	NM	NM	NM	NM	
7. Dec03R9D2								163
Pre- Irrad.	5.4	19.8	10.2	6-1	10.0	4-3	2.70	
Post- Irrad.	5.2	13.5	10.3	6-1	10.2	4-3	2.60	

*Note: Chip processing changed from protiated methanol (CH3OH) to deuterated methanol CD3OD).

Eight protocols were used by SNDP to align the polarization of PBM Sample Sets. As an example, four poling profiles (P-1 through P-4) are shown in Figure 6 illustrating the varying time, temperature and applied voltages used in poling the majority of the samples (the remainder of the profiles are shown in Appendix A.1). All PBM devices in sample set 2 were poled using the P-1 profiles shown in Figure 6(a) as were samples 4 and 5 in Table 5. Samples 3, 6 and 7 in Table 5 were poled using the P-3 profile, while samples 1 and 2 were poled using protocols P-2 and P-4, respectively.

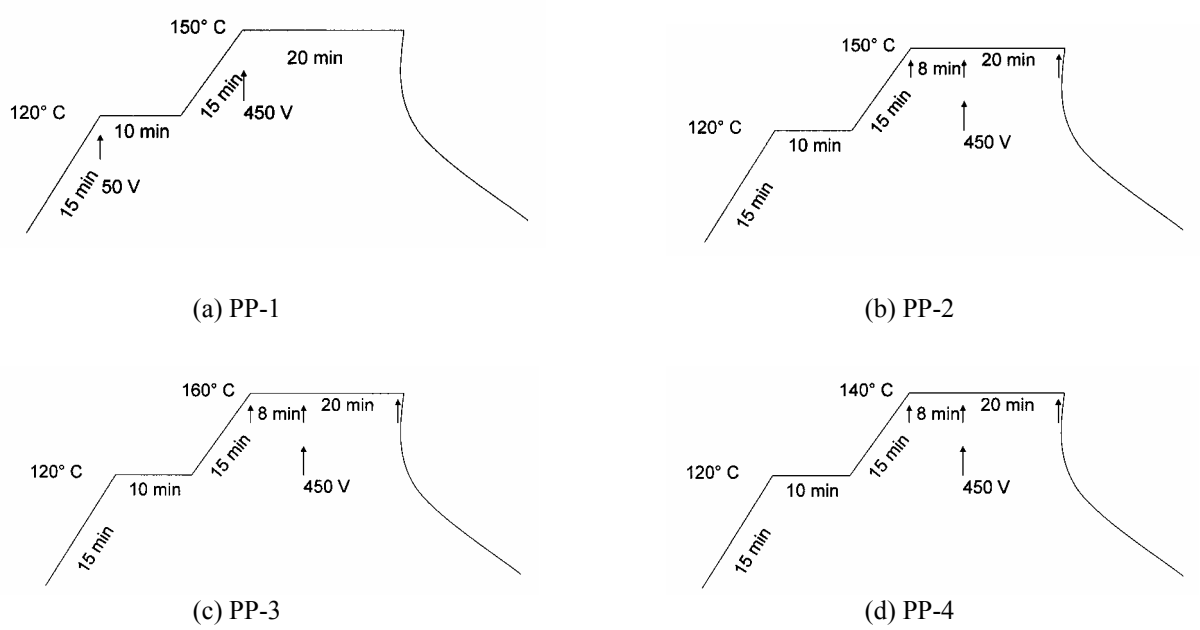

Figure 5. Poling Profiles for SNDP PBMs. Prior to poling, the chips were heated in a vacuum oven at 40 ºC for approximately 3 hours. All devices were stored in air and protected from exposure to light.

Figure 6 depicts the gamma-ray induced changes to the PBM devices shown in Table 4 for Sample Set 2. In all graphical representation of the SNDP data, the multiple pre-irradiation measurements were averaged for comparison to the post irradiation data.

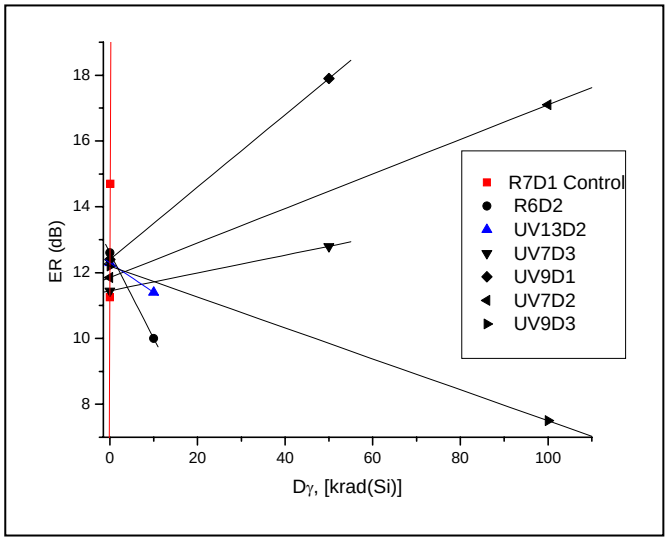

Figure 6. ER responses of irradiated SNDP Sample Set 2.

In Figure 6, the post- irradiation ER values were observed to change by a maximum of +5.25 dB at D_γ = 50 krad(Si) to a minimum of -4.7 dB at D_γ = 100 krad(Si). The post-irradiation ER of the non-irradiated Control sample was observed to also increase by +3.45 dB, indicating that aging processes were occurring in the control and irradiated samples, or, the scatter in the data may have reflected a measure of uncertainty in performing the ER measurements. Since the EO chromophores are known to be light-sensitive, photo-induced chemical changes were believed to have occurred during the brief period that the devices were exposed to light for performing characterization measurements prior to the gamma-ray irradiations. Trapped oxygen in the polymer layers may have been activated resulting in deterioration and destruction of the chromophores. Most likely all these processes were present to some extent indicating that the ER of the devices in Sample Set 2 were not seriously affected by the moderate gamma-ray dose [D_γ = 100 krad(Si)], but rather by environmental conditions.

The small V_π changes (ΔV_π) observed for the irradiated devices comprising Sample Set 2 and shown in Table 4 and in Figure 7 again suggest that the PBMs comprising the

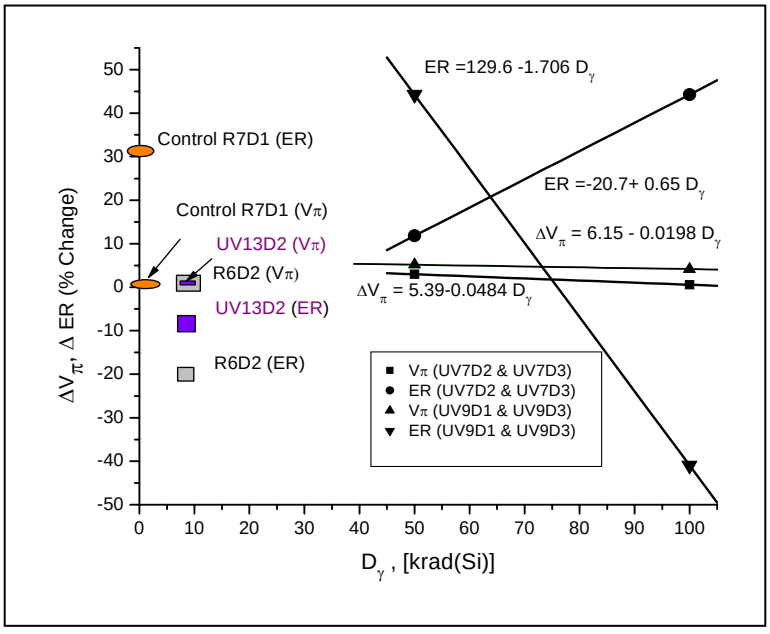

Figure 7. V_π and ER responses of irradiated SNDP Sample Set 2.

irradiated sample set were quite resistant to the gamma-rays to a total dose D_γ = 100 krad(Si).

Figure 7 also illustrates curve-fits to the experimentally measured values of two sets of paired devices. The pre-and post- irradiation data points are expressed in relative (%) changes as ΔV_π and ΔER. The slopes of the ΔV_π curves differ by approximately a factor of 2.4 {i.e.: ΔV_π = -0.019 % [krad(Si)]$^{-1}$ and -0.048% [krad(Si)]$^{-1}$} indicating high resistance to gamma-rays within the measurement uncertainly of the experiment. The ΔV_π and ER responses of unpaired PBMs as well as the responses of the control device are also shown in Figure 5 and are comparable in response to the paired devices. However, the ER changes are shown in units of % changes and are small compared to the magnitude of the dB changes in the individual devices.

Figures 8 and 9 show the pre- and post-irradiated ER and ΔV_π responses of AFRL/SNDP PBMs Sample Set 3. Unlike the devices in the first two sample sets which received varying doses, all devices in Sample Set 3 were irradiated to a single gamma-ray total dose of 163 krad(Si).

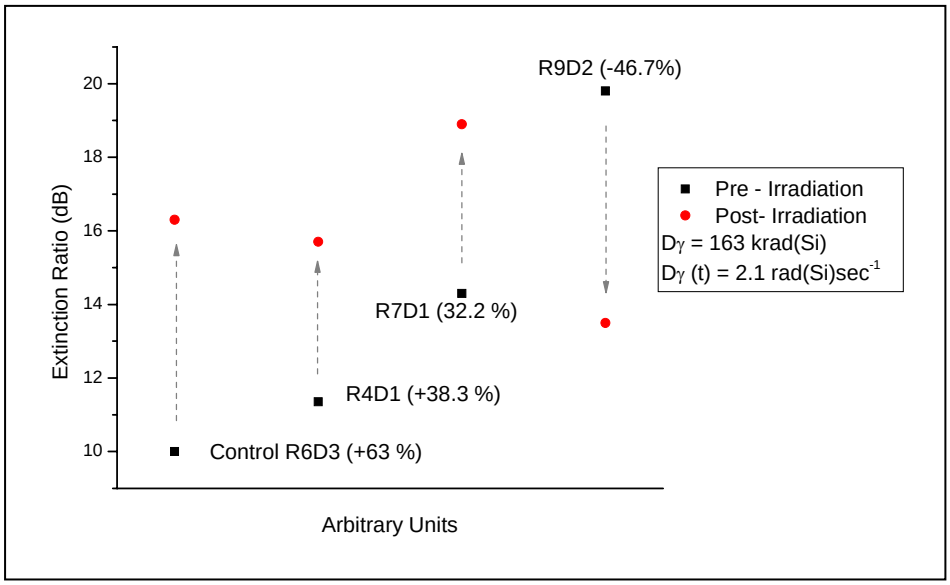

Figure 8. ER responses of irradiated SNDP Sample Set 3. Following irradiation or each device to a total dose D_γ = 163 krad(Si), the irradiated and non-irradiated control PBM samples show mixed ER responses.

In Figure 8, the ER responses following irradiation were similar to the responses noted in Sample Sets 1 and 2. The large relative increase in ER (63%) for the non-irradiated Control sample is again indicative of the presence of aging processes and perhaps measurement uncertainties in the recorded data.

The data in Figure 9 suggests that irradiation of the PBMs in Sample Set 3 to a gamma-ray total dose of 163 krad(Si) resulted in little or no effect of the ionizing radiation in degrading the device V_π values within the uncertainty of the measurements and the suspected deterioration of the devices due to environmental factors. All irradiated devices as well as the non-irradiated Control device exhibited small decreases (i.e. %) in V_π between pre- and post-irradiation measurements. With the exception of device R7D1, three samples changed by $\Delta V_\pi = 0.4$ V. The data in Figure 10 is consistent with similar results observed in Sample Set 2.

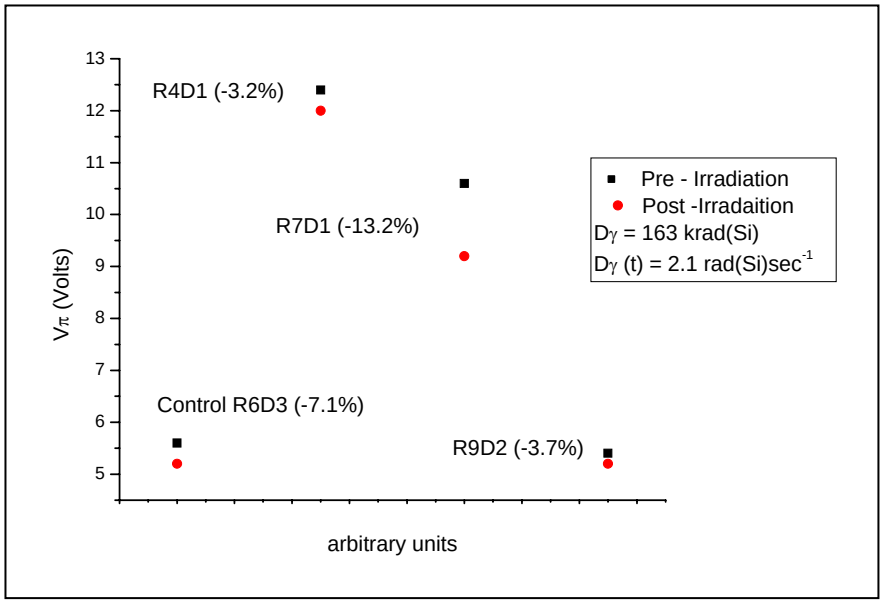

Figure 9. Pre- and post- irradiation V_π responses for SNDP Sample Set 2. Data suggests that V_π of AFRL/SNDP CPW-1/APC modulators are reasonably radiation resistant to gamma-rays at a total dose of $D_\gamma = 163$ krad(Si).

Figure 10 illustrates the mask geometry used to identify straight waveguide sections for the PBMs listed in Tables 4 and 5. The waveguides were composed of 4 μm and 6 μm widths and varied in length between 2 and 3 cm. All data shown has been normalized

relative to 1 cm. The waveguide losses shown in Tables 4 and 5 include losses incurred for signals injected via the polarization maintaining optical fiber butt input signal-coupling and out-coupled signal measurements shown in Figure 4. Intrinsic waveguide propagation (absorption) losses are also included. Thus, as shown in Tables 4 and 5, the total insertion loss (IL, dB/cm) reflects the sum of all known losses.

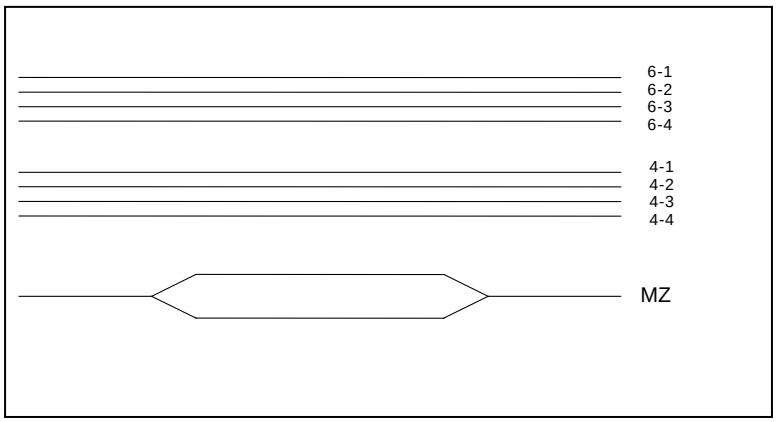

Figure 10. Mask used for fabricating SNDP MZ-PBMs and straight waveguide chips.

In Figure 10 the mask used for fabricating straight waveguides with 4 and 6 μm widths as well as MZ PBM-chip devices is shown. MZ-PBMs fabricated with 1 and 2 cm interaction lengths are identified in Tables 2-5. PBMs devices (D) with 1 cm MZ interaction lengths are identified as D1 and D5 while devices with 2 cm MZ interaction lengths are designated as D2, D3, and D4. The devices identified as D1 or D5 had straight waveguide lengths of 2 cm and Devices D2, D3 and D4 had straight waveguide lengths of 3 cm. The waveguides were designated as 6 μm (1,2,3,4) and 4 μm (1,2,3,4) as shown in Tables 4 and 5.

The PBM chip locations on the wafer is shown in Figure 11, illustrating that the sample set for the irradiation studies consisted of chips originating from 5 areas on the wafer.

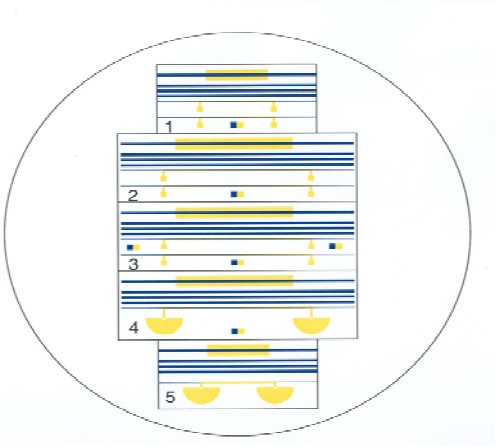

Figure 11. Chip identification and mask location on wafer.

Shown in Figure 12 are the straight waveguide responses for Sample Set 2. The suppression of waveguide losses for all UV-samples at low dose is evident. Both 4 and 6 μm width UV sample waveguides "bottom out" and then begin to degrade- back towards -

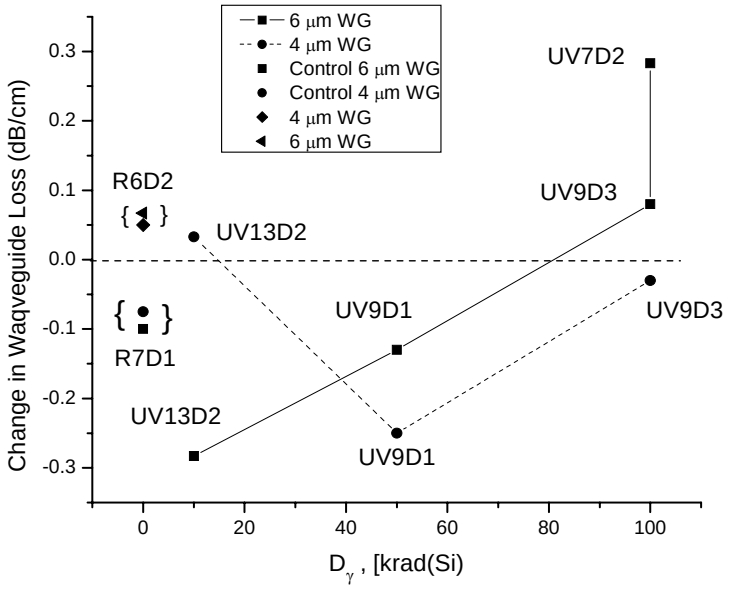

Figure 12. Waveguide responses for Sample Set 2. Solid and dashed lines depict 6 and 4 μm paired waveguide responses, respectively.

pre-irradiated baselines as illustrated by the linear growth curves for sample pairs UV9D1 and UV9D3. The non-irradiated Control device also shows a slight decrease in waveguide loss while the R6D2 device is seen to degrade at low dose.

Figure 13 examines the linear response portion of the 4 μm wide straight waveguide UV9D1 and ?UV9D3 samples show in Figure 12. In Figure 13, α_m is the slope of the fitted curve and represents the relative gamma-ray induced degradation growth rate for the paired sample and is given as $\alpha_m = 4.4 \times 10^{-3}$ dB·cm^{-1}(D_γ)$^{-1}$, where D_γ is expressed in units of krad(Si).

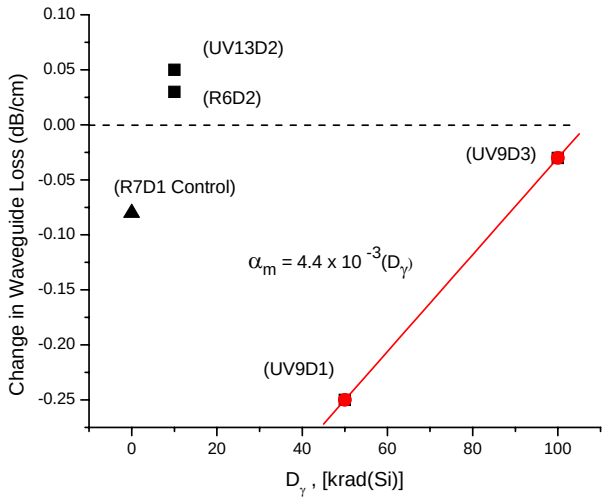

Figure 13. Effect of gamma-rays on 4 μm width waveguides.

Examination of the paired sample responses show an initial decrease (~ 0.25 dB·cm^{-1}) in the UV9D1 waveguide loss at a dose of 50 krad(Si) followed by a smaller decrease (~ 0.03 dB·cm^{-1}) in waveguide UV9D3 loss at a total dose of 100 krad(Si). These limited data indicate that under gamma-ray irradiation, the propagation losses in the paired waveguide samples was initially diminished at a dose of 50 krad(Si), but then increased at higher dose. However, as discussed previously the initial occurrence of trap filling by free carriers originating during the irradiation process may have occurred thereby reducing the scattering and absorption losses associated with inherent defects within the waveguides. This does not however preclude an increase in waveguide propagation losses

at higher dose. To rigorously ascertain the exact mechanism or accurately quantize the magnitude of competing trap-filling and defects caused by the ionization processes, over the dose range of interest, an *in situ* measurement would be required [8, 9].

As shown in Figure 14, the responses of irradiated 6 μm wide straight waveguide samples also resulted in linear growth curves for waveguide losses at increasing dose. Similar

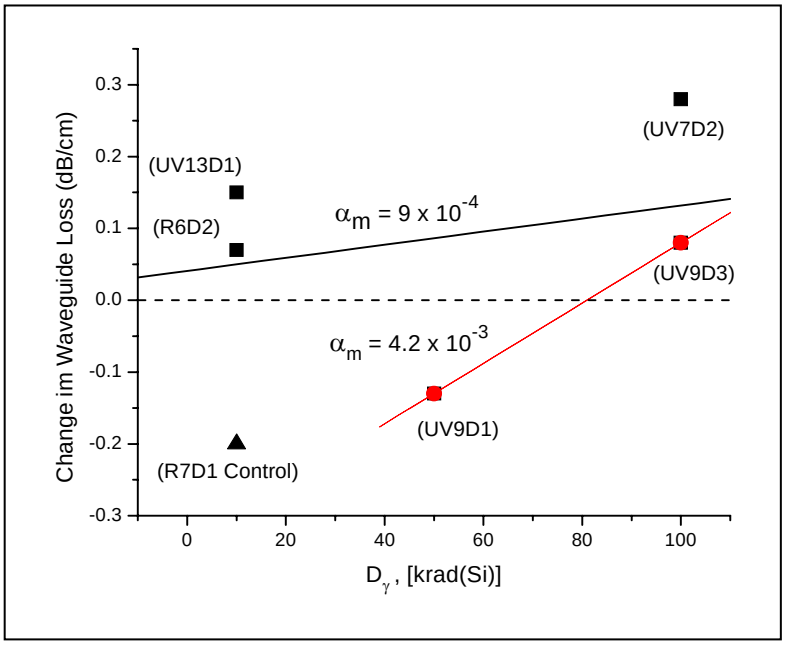

Figure 14. Effect of gamma rays on 6 μm width- ridge waveguide losses.

to the loss behavior observed for the paired 4 μm waveguide samples (shown in Figure 12) the post-irradiation response data for UV9D1 and UV9D3 waveguides suggest that the 6 μm waveguides also experienced an initial decrease in propagation loss ~[at a dose of ~50 krad(Si)] , followed by increased propagation loss at 100 krad(Si). Also shown in Figure 13 is the fitted linear growth curve for the entirety of the irradiated 6 μm waveguide ensemble (fit includes unpaired devices but excludes the non-irradiated control device R7D1). The curve fit for the irradiated ensemble predicts long-term gamma-ray induced degradation to the propagation loss estimated at a rate of α_m = ~ 9 x 10^{-4} dB·cm^{-1} $[D_\gamma]^{-1}$.

Figure 15 illustrates the similarity of radiation induced responses for the differing waveguides located on the same chip and chips located on different regions of the wafer (i.e. regions 1 and 3) as shown in Figure 11. As can be observed, α_m is nearly equivalent

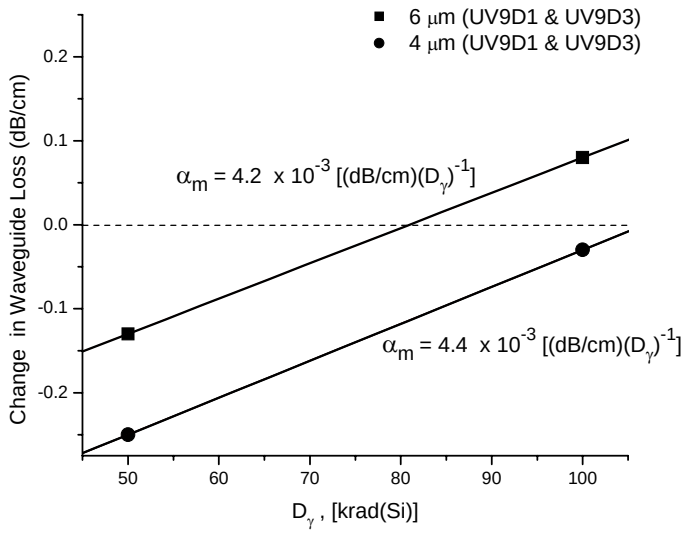

Figure 15. Gamma-ray induced waveguide degradation rates.

for the 4 and 6 μm width waveguides originating from chips UV9D1 and UV9D3. These data strongly indicate very good waveguide uniformity in these two devices which were both poled to a maximum of 450 V and 150 ºC using the poling profile P1 shown in Figure 5(a). Assuming that the linear growth of damage is valid for much higher doses, the post-irradiation waveguide loss ($\Delta\alpha$) curves for devices UV9D1 and UV9D3 shown in Figure 14 are

$$\Delta\alpha = 0.34 + 0.0042\ D_\gamma \qquad (3)$$

and

$$\Delta\alpha = 0.47 + 0.0044\ D_\gamma \qquad (4)$$

for the 6 μm and 4μm waveguides, respectively. For example, the *change* in total propagation loss for the 4 μm waveguides at D_γ = 1000 krad(Si) may be calculated using Equation (4) to be $\Delta\alpha = 5.17\ dB{\cdot}cm^{-1}$.

Shown in Figure 16 are the straight waveguide change in loss responses for gamma-ray irradiations preformed at D_γ = 163 krad(Si). While the Control sample decreased in its

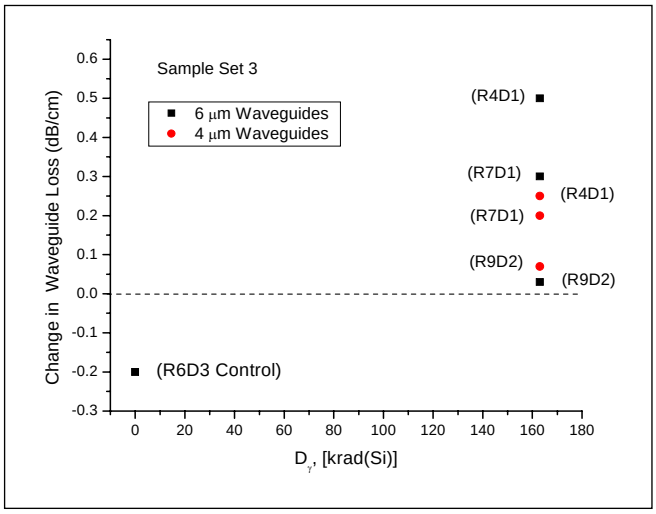

Figure 16. Comparison of straight waveguide losses at 163 krad(Si) total dose.

loss, the irradiated waveguide samples change in waveguide losses ranges from 0.033 to 0.5 dB·cm^{-1} with higher losses exhibited by the 6 μm width - 2 cm length waveguides. Since the sample set was small it is not possible to conclusively determine a physical reason for the difference in losses between the differing waveguide sizes.

RESPONSES OF IRRADIATED AFRL/MLPSO NLO DNA EO MATERIALS

A blend of salmon deoxyribonucleic acid (DNA)-hexadeCetylTriMethylAmmonium Chloride (CTMA) film samples characterized and provided by AFRL/MLPSO were studied for their spectral responses following irradiations over the spectral range λ = 240-2600 nm. Shown in Table 6 are the irradiation conditions. The influence of low energy

Table 6. MLPSO samples and irradiation conditions.

Material Sample / Device	Gamma-Ray Dose (D_γ) [krad(Si)] (±10%)	Temperature (^oC)
Biopolymer DNA/Lipid Complex (CTMA)- Coated Glass Substrates		
DNA/CTMA 1	104	18.9 +/- 0.5
DNA/CTMA 2	50.6	18.4 +/- 0.5
DNA/CTMA 3	9.60	18.9 +/- 0.5
DNA/CTMA Control	N/A	18.9 +/- 0.5

gamma-rays (predominant photon energies of 1.173 and 1.332 MeV) on the spectral response of three NLO DNA samples is shown in Figure 17. The NLO thin film polymer

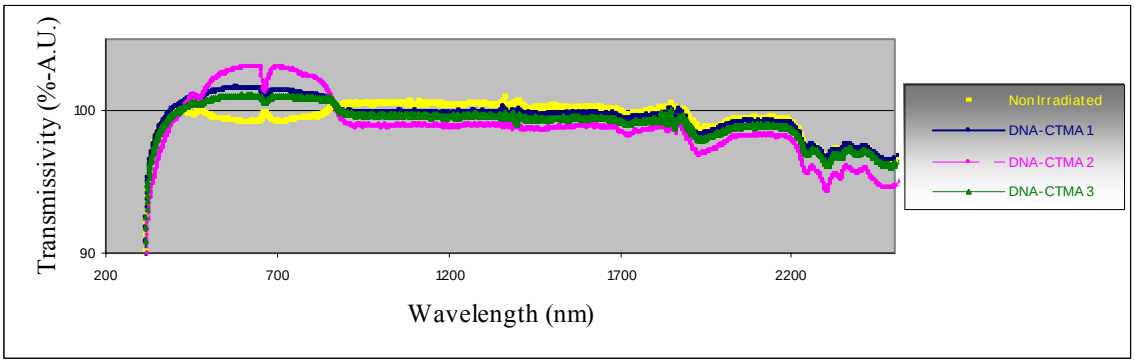

Figure 17. Post- irradiation transmission spectra of DNA/CTMA films.

samples consisted of a blend of DNA/CTMA films ranging in thickness from 7.0 – 9.1 μm on borosilicate glass slides. CTMA lipid was used to replace the sodium cation of the DNA by an ion exchange reaction. Figure 16 depicts the pre- and post- irradiation transmission spectra of DNA/CTMA films over the spectral range of 240 -2600 nm. The ^{60}Co gamma-ray average dose rate used in all DNA/CTMA irradiations was 1.91

rad(Si)·sec^{-1}. As may be observed, the transmissivity responses of the irradiated films do not linearly scale with dose. For wavelengths $\lambda > \sim 882 - 2600$ nm, a small reduction in the transmissivity is evident. Contrarily, an increase in transmissivity is observed for $\lambda =$ 240 - 882 nm. Fluorescence measurements performed at AFRL/MLPSO on similar DNA/CTMA films have also shown a similar transmissive response behavior dependent on the amount of dye concentration introduced within the films.

Ladder-like double helix DNA in various solutions is known to readily deform under room temperature conditions from an ideal straight and elongated structure into random-coil configurations and reported fluorescence-polarization studies have revealed the presence of a twisting elasticity that leads to significant structural deformations [16, 17]. Monoenergetic X-ray induced K-shell ionization of DNA or DNA constituents (i.e. bromine and ATP) in solution have been studied and it was reported that significant degradation occurred with only a modest increase (< 1%) in the photon energies [18, 19]. However, there is no data to suggest that this reported behavior can be confidently applied to interpreting the solid state DNA EO thin film responses shown in Figure16. Nor does the data presented herein rule out the possibility that NLO properties unique to the DNA solid films might also be susceptible to low-dose radiation induced degradation, since only spectral data is presented. However, in yet another reported study, the possibility of strand breaks in solid state - plasmid DNA induced by K-shell (X-ray) ionization of bromine incorporated into the DNA were investigated but were reported not to occur [20]. In contrast to this latter study, the data shown in Figure 17 for the DNA/CTMA thin films indicate a remarkable change in the transmissive spectra of the thin films by scaling in a nonlinear fashion with applied gamma-ray dose. This could indicate that the other optical properties of the DNA/CTMA material might respond in some complex manner under equivalent dose and dose rate conditions.

RESPONSES OF IRRADIATED COMMERCIAL PBMS

PBM devices for the gamma-ray irradiation studies were provided by Pacific Wave Industries (PWI), IPITEK Inc. (IPITEK) and Nanosonic Inc. (NS). Comparison of the response data within the device provider sample sets should be approached with caution, since pre- and post-irradiation measurements were independently performed by each of the sample providers using varying measurement techniques. Factors which must be considered in comparisons also include variables such as age of the device, the extent of elapsed time between pre- and post- irradiation measurements, device storage conditions, launched light intensities, exposure to background light intensities and exposure times. These and other unknown variables can factor into skewing comparison of the results.

Shown in Figure 18(a) is an illustration of the PWI MZ modulator, composed of CLD-75/ APC and cladding materials.

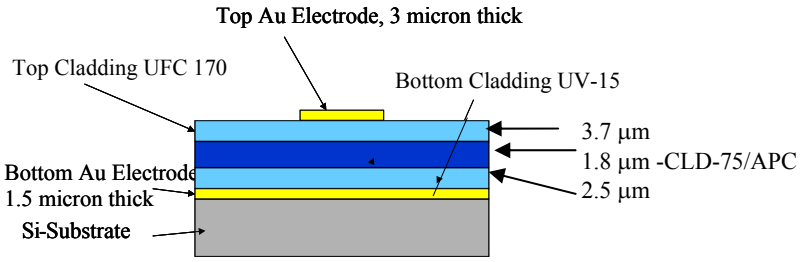

(a)

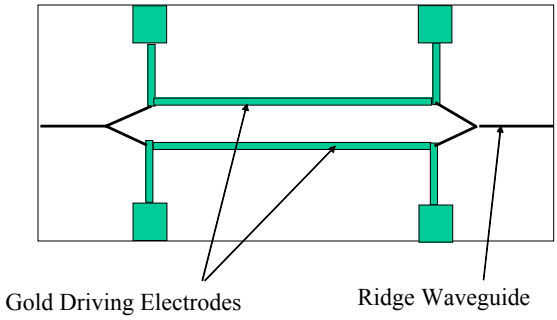

(b)

Figure 18. PWI-MZ PBMs. Cross-section (a) and (b) top view of electrodes on 4 µm width ridge waveguides are shown.

Figure 18(b) illustrates the top view of the modulator. The polymer layers were spun-on, metals were e-beam deposited or electroplated, and the waveguides and electrodes were defined by photolithography, reactive ion etching and wet etching. The devices were poled by electrode poling at 500 V and a temperature of 145 ºC. Shown in Table 7 are the device responses over a gamma-ray total dose of D_γ = 104 krad(Si).

Table 7- Gamma-ray irradiation response data for PWI PBMs.

PWI Sample No.	γ-ray Dose [krad(Si)]	p^+ Dose [krad(Si)]	$V_{\pi\,(Pre\text{-}Irrad)}$ $V_{\pi\,(Post\text{-}Irrad)}$ (Volt) *(%Change)*	Absorption Loss** (dB/cm) *(dB/cm-Change)*	$ER_{(Pre\text{-}Irrad)}$ $ER_{(Post\text{-}Irrad)}$ (dB) *(dB-Change)*	$r_{33(Pre\text{-}Irrad)}$ (pm/V)	$r_{33(Post\text{-}Irrad)}$ (pm/V) *(%Change)*
PWI-1	51.4	N/A	7.5 7.06 *(- 5.9%)*	6.17 5.91 *(--0.26)*	22.2 20.1 *(-2.09)*	23.6	25.07 *(+6.2)*
PWI-2*#	104	N/A	7.65 11.56* *(+51.%)*	6.27 6.16 *(-0.11)*	22.8 18.7* *(-4.08)**	23.2*	15.35* *(- 34)**
PWI-3	9.6	N/A	7.34 7.04 *(- 4.08%)*	6.27 5.7 *(-0.57)*	22.4 19.6 *(-2.79)*	24.14	25.3 *(+4.8)*
PWI-4*	***Control Sample (C)***		7.18 *10.3** ***(+43.6%)****	6.42 6.37 *(-0.05)*	24.1 18.7* *(-5.4)**	24.68*	17.18* *(- 30)**
PWI-5	N/A	10	Data Not Provided				
PWI-6	N/A	50					
PWI-7	N/A	99.9					

* Visible damage to driving electrodes incurred prior to or after irradiations.
** Absorption loss includes material loss and waveguide loss

The data in Table 7 illustrate that sample PWI-1 experienced a decrease (-0.44 V) in its half wave voltage at D_γ = 51.4 krad(Si) while sample PWI-3 also experienced a decrease from its pre-irradiated V_π value following irradiation at D_γ = 9.6 krad(Si). The non-irradiated Control sample and sample PWI-2 irradiated to a high dose of 104 krad(Si) experienced damage to their electrodes caused by handling or during transit thereby causing their effective lengths to be reduced compared to their design (interaction)

lengths of 1.5 cm. The damage to the electrodes resulted in large reductions in the calculated r_{33} coefficients since all r_{33} values were calculated using Equation (1) and an interaction length of L= 1.5 cm. The pre-irradiated device V_π values ranged from 7.18-7.65 V and for the two devices (PWI-1 and -3) which had fully operational electrodes, and the change in these values was observed to decrease with increasing gamma-ray

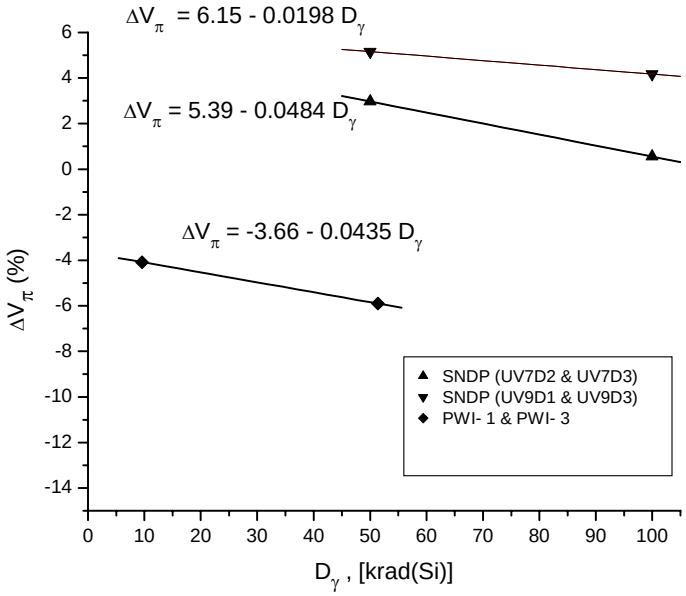

Figure 19. Comparison of SNDP and PWI ΔV_π post-irradiation responses.

dose. The gamma-ray-induced changes in V_π values observed for the CLD-75/APC devices was similar to the SNDP CPW-1/APC responses as evidenced by the slopes of the linear regression curves. In Figure 19, the half-wave voltages in the SNDP and PWI devices appear to consistently decrease with increasing dose indicating that the conductance of the polymer based devices increased with increasing dose. While all devices shown in Figure 19 were fabricated using similar cladding materials, there were variations between the SNDP and PWI devices in regards to their individual core materials, cladding thickness, electrodes and poling conditions. Regardless, the minimal responses of these low V_π devices show excellent potential for withstanding gamma-ray irradiation at much higher dose. However, a significantly larger number of devices subjected to higher total dose would be required to verify this behavior under passive

irradiation conditions. The use of *in situ*-dynamic irradiations would facilitate a temporal study of the irradiation process over a wide dose range and require fewer samples to carefully examine the exact onset and persistence of the various PBM response behavior.

As shown in Figure 20 the absorption loss in the PWI modulator samples was observed to initially decrease at low dose and then increase with increasing dose. All PWI devices were 2.2 cm in length and the absorption loss measured and reported by PWI included both material and coupling losses.

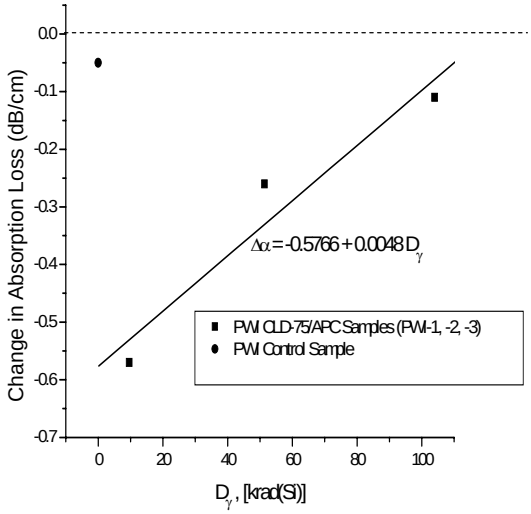

Figure 20. Suppression of absorption loss in gamma-ray irradiated PWI-PBMs.

As can be seen in Figure 20, the absorption/insertion loss in the non-irradiated Control sample decreased only slightly (0.05 dB) compared to the decreases observed in the irradiated devices. A linear growth curve was fitted to the irradiated data resulting in a slope of $\alpha_m = 4.8 \times 10^{-3}$ dB $\{cm \cdot [krad(Si)]\}^{-1}$. This behavior and the order of the loss was consistent with the SNDP waveguide absorption data observed previously and shown in Figures 12-14 where the SNDP waveguides losses were shown to initially decrease at a dose of $D_\gamma = 50$ krad(Si) and were followed by a linear growth in loss at higher dose.

Post-irradiation PWI PBM extinction ratio responses are shown in Figure 21. The data and linear regression curve fit to the data lies well above the large degradation noted for

the non-irradiated Control sample ER response. Additional samples and irradiations at increased dose would be required to verify whether the ER decrease in the irradiated PWI PBMs are predominantly driven by ionizing radiation effects or other processes such as aging (as is indicated by the ER response of the non-irradiated Control device).

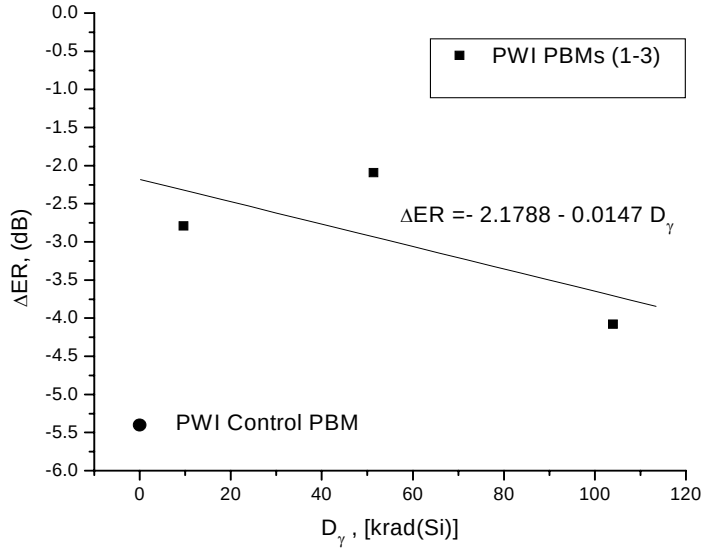

Figure 21. ER responses of irradiated PWI-PBMs.

IPITEK provided PBMs based on LD3 and CLD core layer materials for gamma-ray and proton irradiation studies. LD3 was composed of PMMA containing 4-[bis(2-hydroxyethl)amino]-4'-[(methylacryloyl-hxyl)sufonyl] azobenzene chromophores. Figure 22 shows a diagram of the LD3-based MZ-062 and MZ-063 samples fabricated by spun-on, self assembly and photolithographic techniques. MZ-062 was poled at 53V/μm and 124 ºC, while MZ-063 was poled at 44V/μm and 124 ºC. The pre- and post-irradiation measurements for the devices are shown in Table 8. Two pigtailed modulators (I MZ and II MZ) were also irradiated by gamma-rays, however, the ceramic couplers were believed damaged by handling and following irradiation showed color changes and failed to operate during the post-irradiation characterizations. The ceramic was believed to be predominantly composed of hydrous aluminum silicate and most likely color centers were formed during the irradiation as well as shrinkage due to volumetric changes thereby causing stresses that potentially resulted in connector failure.

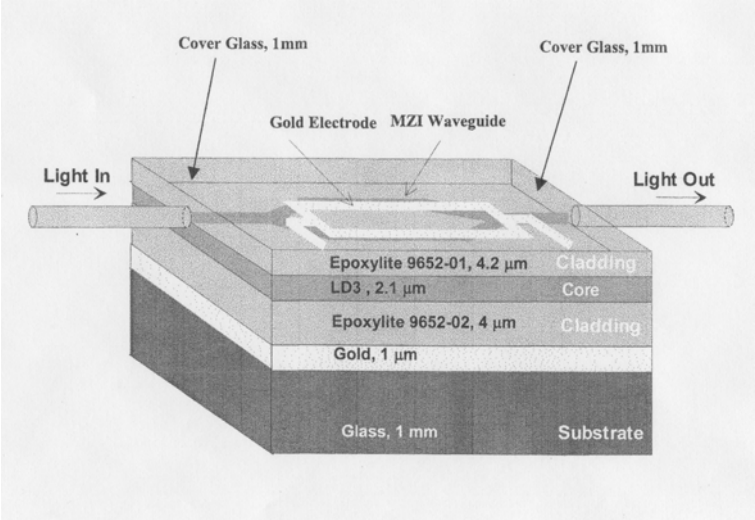

Figure 22. Cross-section of IPITEK MZ-063 and MZ-062 PBM chips.

Table 8. Gamma-ray and proton irradiation response data for IPITEK PBMs.

IPITEK Sample No.	γ-ray Dose [krad(Si)]	p^+ Dose [krad(Si)]	$V_{\pi\ (Pre-\ Irrad)}$ $V_{\pi\ (Post-\ Irrad)}$ (Volt) (% change)	$IL_{(Pre-\ Irrad)}$ $IL_{(Post-Irad)}$ (ΔdB/cm)	Pre-Irrad. r_{33} (pm/V)	Post-Irrad. r_{33} (pm/V) (% change)
1. MZ 062	102	N/A	20 25 (+25%)	16 18.6 (+2.6)	20	25 (+25%)
2. MZ 063	49.9	N/A	26 20 (-23%)	20.3 18.5 (-1.8)	26	20 (-23%)
3. MZ 100	N/A	100	5.78 6.66 (+15.2%)	20.5 21.5 (+1.0)	5.78	6.66 (+15.2%)
4. I MZ*	100	No Data: Pigtailed PBMs experienced breakage at coupler connections & radiation-induced color changes in the ceramic based connectors				
5. II MZ*	100					

*Note: Pigtailed with 3M-PMF and SMF-28

As shown in Figure 23 the LD3 devices were composed of a main chain polymer with epoxylite claddings differing from the SNDP and PWI devices. Compare to SNDP PBM responses shown in Tables 4, 5and 7 the IPITEK PBM responses shown in Table 8 for the pre- and post–irradiation values for V_π and are substantially larger. However, IPITEK

reported that their response data did lie within the uncertainty of their measurements. Figure 23 compares the post-irradiation change in half-wave voltage responses of the paired IPITEK PBMs with SNDP and PWI PBMs. The two IPITEK irradiated devices were noted to have substantially higher V_π values (i.e. 20 and 26 volts) compared to the SNDP and PWI PBMs, suggesting less poling stability.

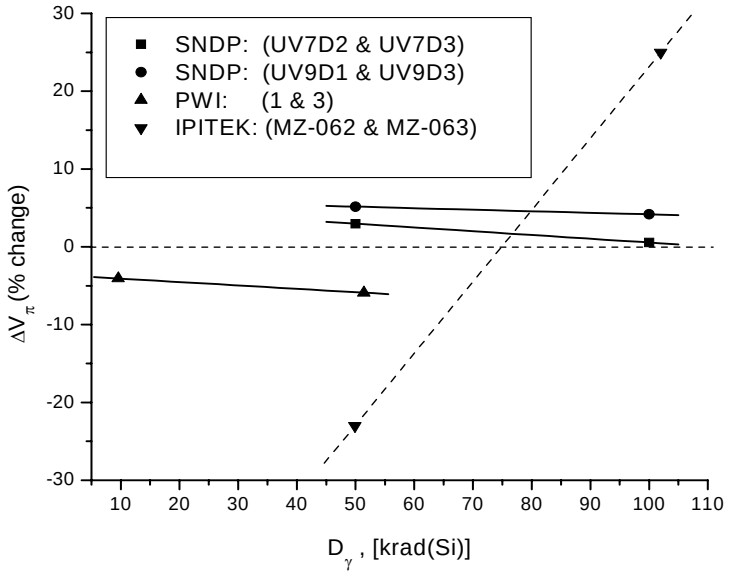

Figure 23. Comparison of SNDP, PWI and IPITEK post-irradiation ΔV_π responses.

Due to the 20% uncertainty in the IPITEK measurement of ΔV_π and the limited number of devices in the sample set, it is difficult to compare with confidence the ΔV_π response of the IPITEK devices relative to the other SNDP and PWI samples shown in Figure 22. The large changes in the device ΔV_π responses are consistent with previously reported data asserting that strongly poled PBMs exhibiting V_π voltages in the range of a few volts, are less likely to undergo large changes to their half-wave voltages during gamma-ray irradiation [1].

Figure 24 compares the change in absorption/insertion losses of the IPITEK paired devices with SNDP and PWI paired devices. While losses for the SNDP and PWI devices composed of CPW-1APC and CLD-75/APC materials coincide quite well, the IPITEK

LD3 based device showed a greater rate of degradation. Because of the extent of uncertainty in the IPTEK measurements, caution should be exercised in interpreting these results. The possibility exists that the extent of degradation exhibited in the IPITEK

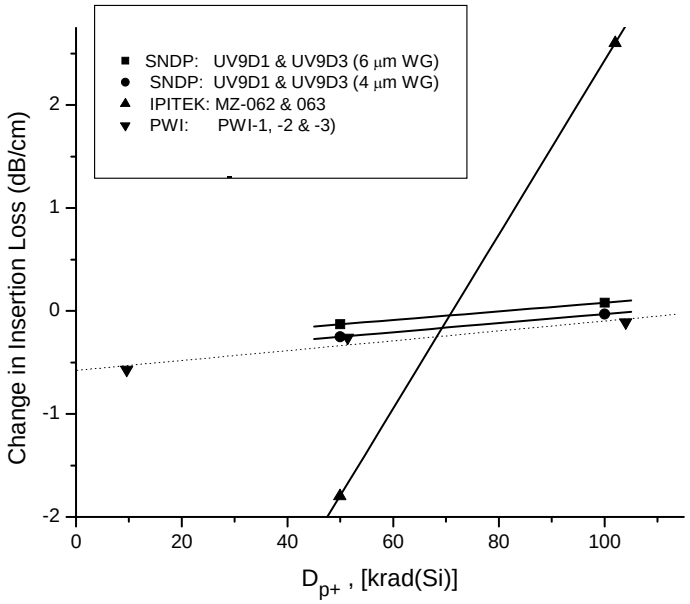

Figure 24. Comparison of insertion losses in SNDP, PWI and IPITEK PBMs.

devices was similar to losses observed in SNDP and PWI devices but are not resolvable due to the measurement uncertainty. In situ measurements would provide a means to quickly resolve certain of the measurement uncertainties.

Hybrid PBMs consisting of an active region fabricated with self assembled PCBS and a spun-on NLO thin film were provided by NS for gamma-ray irradiations. Initially, hybrid trench waveguide devices were fabricated, however, serious de-lamination of adjacent thin film layers especially during the chip dicing operation precluding their inclusion in the irradiation studies. This design was abandoned and, the PBM design shown in Figure 24 using a 100 nm thick PCBS layer was used to produce six devices. However, in the final fabrication steps, “star” cracks in the device optical path were noticed in all NS

modulators. The cracks were believed due to have formed during the photo-cure processing.

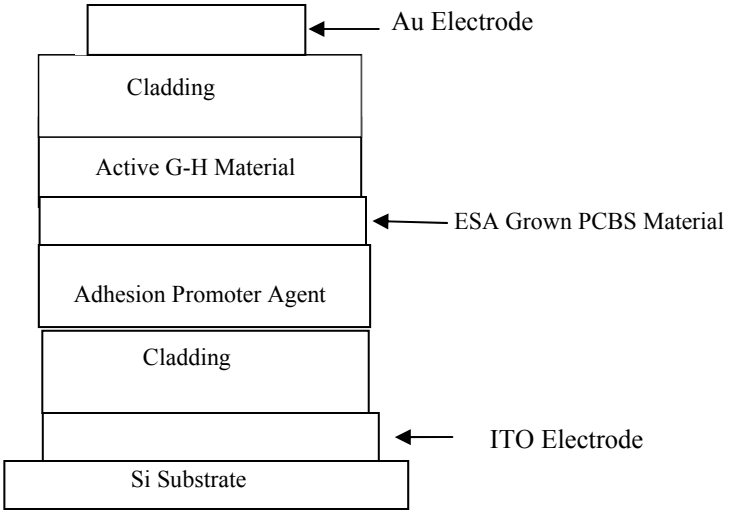

Figure 25. NS hybrid PCBS-based PBM.

Shrinking of the ~2000A active guest host-(G-H) polymer film was believed to have caused stress on the active electrostatic self assembled NS PCBS film layer. These and other related or contributing defects resulted in an increase in light scattering, decreased poling effectiveness and loss of conductance. As shown in Table 9 pre-irradiation measurements revealed high insertion losses for device samples 2-6 and precluded measurements of V_π and ER. However, pre-irradiation measurement of these parameters for sample 1 was accomplished and the device was irradiated to a total dose 152 krad(Si) [1.89 rad (Si) sec^{-1}] at a temperature of 21.8 ºC. Post- irradiation measurements yielded only a questionable measurement of the device insertion loss.

As can be seen in Table 9 the insertion loss measurements for device sample 200311-1 was not stable nor repeatable and resulted in a range of loss values. Figure 25 shows the set up used for measuring the device voltage waveforms. The device exhibited a high pre-irradiation half-wave voltage of V_π = 14V suggesting the presence of non-optimum poling and therefore the conductance of the device was not comparable to the SNDP and PWI PBMs. As discussed earlier, PBMs with high V_π values are very likely to become unstable in the presence of ionizing radiation such as gamma-rays [1].

Table 9- Gamma-ray irradiation response data for NS PBMs.

	Straight Waveguide			MZ PBM					
Samples 200311-	Pre-Poling IL (dB)	Post - Poling IL (dB)	Post-Irrad. IL (dB)	Pre-Irrad IL (dB)	Pre-Irrad V_π (Volts)	Pre-Irrad ER (dB)	Post-Irrad IL (dB)	Post-Irrad V_π (dB)	Post-Irrad ER (dB)
1	15.5-27.5	18.2-28.7	24.4-32.9	36	14	6	*	*	*
2	34.2-44.9	45.1-46.2	**	*Note: Data not measurable (NM) as a result of device fabrication problems, aging, and possibly radiation induced degradation . **Note: Excessive device deterioration and degradation prevented further measurements.					
3	44.0-45.8	**	**						
4	27.8-42.8	**	**						
5	40.7-47.0	42.7-47.1	**						
6	23.7-46.6	29.5-45.6	**						

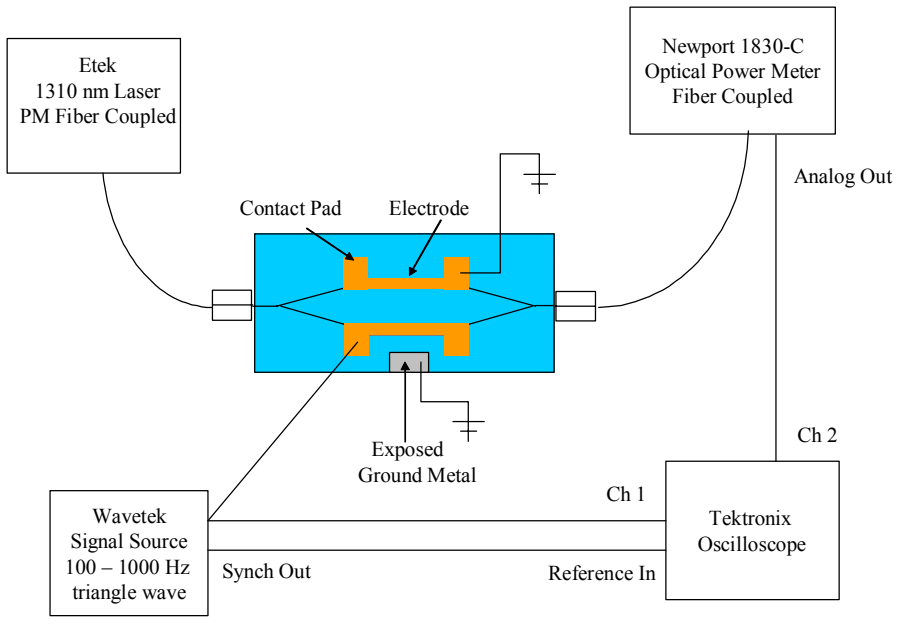

Figure 26. NS apparatus for measuring voltage waveforms.

IRRADIATION OF PBMs BY PROTONS: RESULTS AND ANALYSIS

Passive proton irradiations of SNDP, IPITEK and PWI PBM samples were all conducted at the Crocker Nuclear Laboratory (CNL), University of California, Davis, CA. Figure 27 shows the CNL cyclotron apparatus-beam line that was used to irradiate all devices at a proton energy centered at 25.6 MeV. This proton energy was chosen in order to allow relative comparison of results between the different samples. The proton energy was determined using the SRIM Computer Program to insure that the protons completely traversed the polymer modulator thin film claddings and active EO-core regions thereby being deposited well into the device substrate, or, passed through the device substrate region [21].

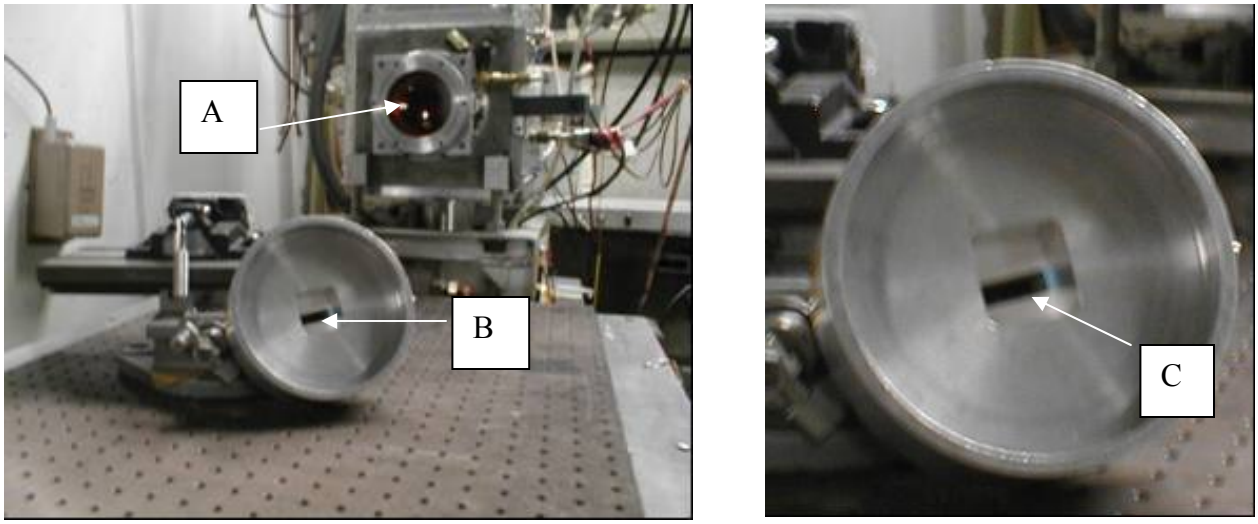

Figure 27. Crocker Nuclear Laboratory set-up for proton irradiations. The output window of the CNL cyclotron is shown in (**A**), while (**B**) shows a typical PBM mounted on a target holder. An enlarged view of the PBM mounted in the target holder is shown in (**C**).

The proton beam was directed at the face side of the modulators (electrode side) as shown in Figure 28. All irradiations were performed at room temperature. Care was taken to insure that the proton beam was centered on the mid-point region between the PBM electrode areas equidistant from the device Y-branches.

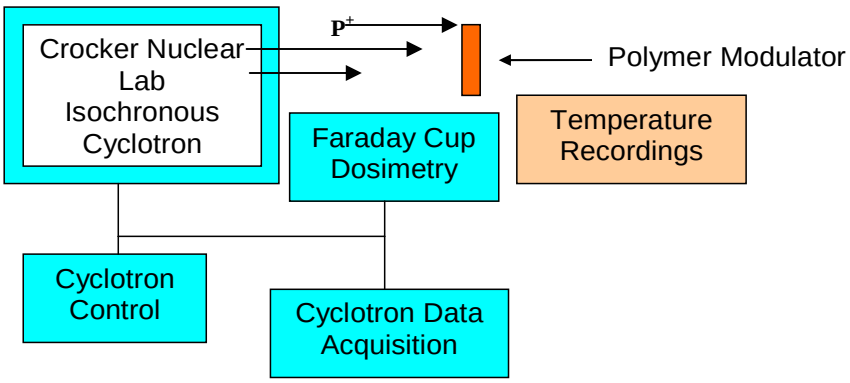

Figure 28. Equipment arrangement for proton irradiation of PBMs.

Shown in Appendix A.2 is a typical dosimetry data sheet showing the fluence, flux, dose and beam-size parameters used in the proton irradiation of PBMs. Since the IPITEK, PWI and SNDP device sizes varied, some caution must be taken in interpreting the device responses. As shown in Appendix A.3, the total dose experienced by each device was carefully controlled. However, larger proton-irradiated chips (>2.5 cm diameter) may not have experienced total exposure of their waveguide sections showing less degradation.

Shown in Table 10 are the PBM sample sets irradiated by high energy (E_{p+} = 25.6 MeV) protons. The IPITEK and PWI irradiations were performed in March 2003, while the SNDP irradiation was performed in November 2003.

Table 10. PBM sample characteristics and proton irradiation conditions.

Sample Set No. & Provider	PBMs Irradiated E_{p+} = 25.6 MeV (No.)	Operational Wavelength (nm)	Proton Fluence 10^{11} p^+ (cm^{-2})	Total Dose [krad(Si)]	Temperature (° C)
4. AFRL/SNDP	3	1550	1.84--3.68	10, 50, 100	23.5
2. IPITEK	1	1550	3.68	100	22
2. PWI	3	1550	1.85-3.68	10, 50, 100	22

The SNDP PBM sample set consisted of 4 APC/CPW-1 samples individually poled at the chip level as described earlier. Of the four devices comprising the sample set, three devices were irradiated and one non-irradiated device served as a control device. IPITEK provided one PBM chip device (MZ-100, CLD-1 active core) for irradiation, while PWI provided three CLD active core devices (Note: post irradiation data was not provided by PWI (see Table 7). The IPITEK device was similar to the IPITEK LD3 devices shown in Figure 21, except for a thicker (4.5 μm) top cladding layer. The CLD- 1 thickness for the IPITEK MZ-100 device was 2.1 μm.

Table 11. Proton response data for in SNDP PBMs (Sample Set 4).

SNDP Sample Set 4 (PBM No.& Measurement - Date)	**V_π (V)**	**ER (dB)**	**6 μm Straight WG (dB)**		**4 μm Straight WG (dB)**		**2 cm V_π Push-Pull Equivalent (V)**	**Dose [krad(Si)]**
1. R8D2								
Pre- irrad. 11/12/03	7.2	11.1	8.3	6-4	8.6	4-3	3.60	
Pre- irrad. 11/13/03	7.0	10.6	7.9	6-4	8.8	4-3	3.50	
Post- irrad. 11/26/03	7.4	9.3	8.1	6-4	9.4	4-3	3.70	50
2. R8D3								
Pre- irrad. 11/12/03	5.2	10.7	8.3	6-1	8.9	4-3	2.60	
Pre- irrad. 11/13/03	5.4	10.8	8.8	6-1	8.7	4-3	2.70	
Post- irrad. 11/26/03	5.7	10.5	8.9	6.1	9.1	4-3	2.85	100
3. UV7D1								
Pre- irrad. 11/12/03	9.4	16.1	7.6	6-3	9.6	4-3	2.35	
Pre- irrad. 11/12/03	9.6	13.5	7.6	6-3	9.5	4-3	2.40	
Post- irrad. 11/26/03	10.2	14.5	8.0	6-3	9.4	4-3	2.55	0- (Control)
4. UV13D1								
Pre- irrad. 11/06/03	11.2	11.7	NM		8.2	4-2	2.80	
Pre- irrad. 11/10/03	11.4	13.4	6.9	6-3	8.3	4-2	2.85	
Post- irrad. 11/26/03	11.4	15.5	7.0	6-3	8.4	4-2	2.85	10

Tables 8 and 11 provide a delineation of the pre- and post- proton irradiation responses of the IPITEK and SNDP PBMs, respectively (see Figure A-5 in APPENDIX A.3 for V_π measurement set-up). Figure 29 provides a comparison of the relative changes in the irradiated sample V_π values where ΔV_π is expressed in % relative to the averaged pre-

irradiation measurements. As may be observed, the data suggests that the half-wave voltage of the SNDP APC/CPW-1 devices scaled linearly with applied proton dose.

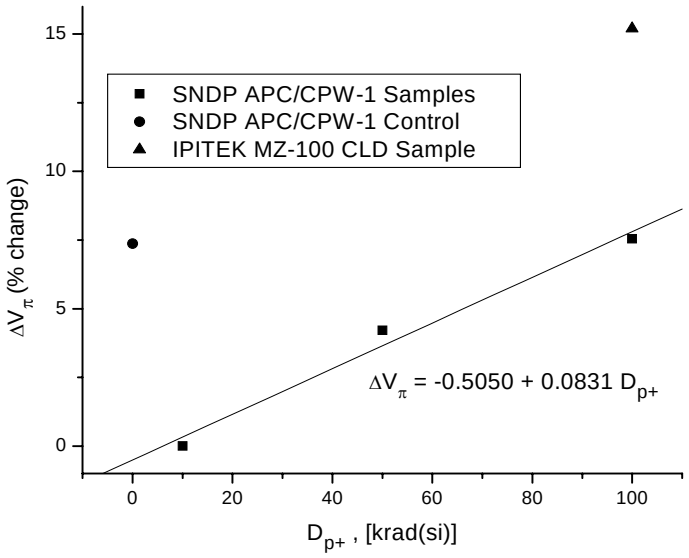

Figure 29. ΔV_π responses for proton irradiated SNDP and IPITEK PBMs.

For example, for SNDP PBM device R8D3 shown in Table 11, the measured increase in the device pre-irradiation average half-wave voltage (V_π = 5.3 V) following irradiation was ΔV_π ~ 7.55 %. As shown in Figure 29, the IPITEK post-irradiation loss response for the single device irradiated was substantially higher.

Data Fusion

It is important to consolidate and compare the relative dose effects in PBMs resulting from the proton and gamma-ray irradiations. In some instances, the radiation induced changes were quite subtle as exemplified by consolidating the data of Figures 19 and 23 with Figure 29 and shown in Figure 30. In Figure 30 are the ΔV_π comparison data for SNDP, PWI, and IPTEK PBMs irradiated by protons and gamma-rays. The SNDP response data for APC/CPW-1 devices are well grouped for both proton and gamma-ray irradiations and show a spread of < 8% change in the half-wave voltage for a total dose of ~100 krad(Si). The PWI and SNDP device responses to gamma-rays show similar degradation slopes even though the core materials differed. The data suggests that SNDP and PWI PBMs which possess low V_π values are reasonably radiation resistant to both gamma-ray and proton irradiations at a total dose of ~ 100 krad(Si). The increased degradation rate observed for the proton responses at equivalent dose (referenced to dose in Si) was attributed to dislocation as well as ionization induced effects.

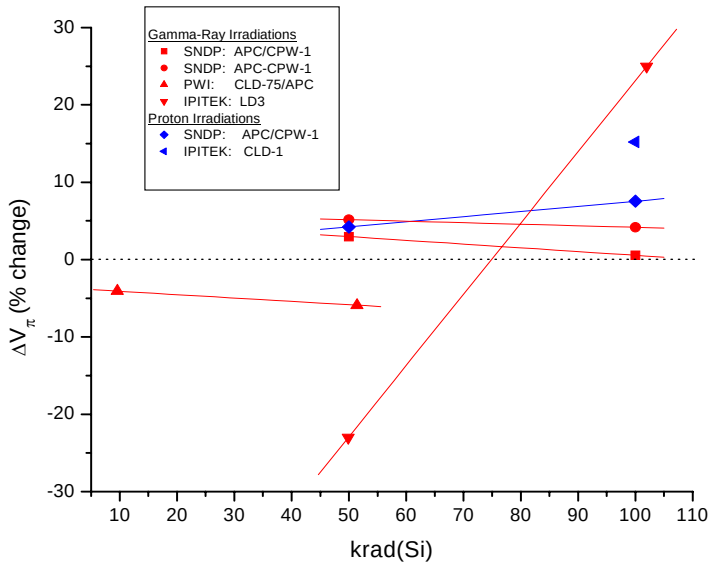

Figure 30. Fusion of gamma-ray and proton induced ΔV_π response data.

Shown in Figure 31 are changes to the insertion losses of SNDP and IPITEK proton irradiated devices. The change in waveguide insertion loss for SNDP devices varied between 0.05 and 0.23 db·cm^{-1} [10-100 krad(Si)] compared to the IPITEK change in

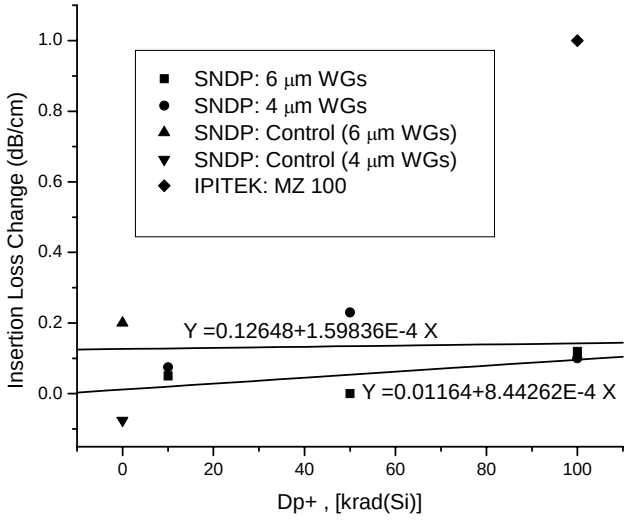

Figure 31. Effects of protons on SNDP and IPITEK PBM insertion losses.

insertion loss of ~1.0 db·cm^{-1} at a total dose of 100 krad(Si). However, unlike the SNDP data, the IPITEK also includes losses through the Y-branch sections. The SNDP 4 and 6 μm width waveguide sample (R8D2, R8D3 and UV13D1) responses varied within ~ 0.18 dB·cm^{-1} over the dose range 50-100 krad(Si) with degradation rates of 1.50836 x 10^{-4} and 8.44262 x 10^{-4} {dB·cm^{-1}[krad(Si)]$^{-1}$} for the 4 and 6 μm waveguide widths, respectively. The data indicates that the device insertion losses are increased in the waveguides following proton irradiations. This behavior contrasts with waveguide responses observed for gamma-ray irradiations, where the insertion losses are initially decreased at low dose. It is interesting to observe that the spread in the non-irradiated control device 4 and 6 μm straight waveguide loss data exceeded the spread in all SNDP irradiated samples. This is an indication that the SNDP devices were also responding to environmental (aging) factors similar to the results observed in the gamma-ray irradiations.

Figure 32 compares the gamma-ray and proton induced changes in the insertion losses of SNDP, PWI and IPITEK paired devices. The data suggests that SNDP devices experience

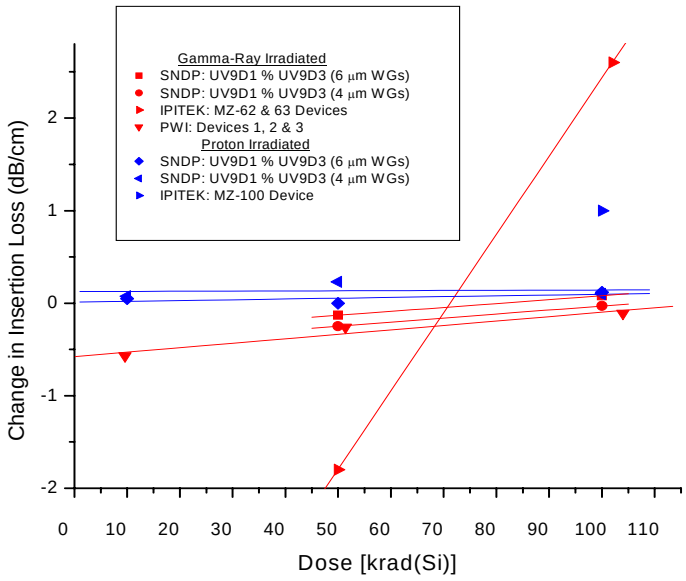

Figure 32. Fusion of PBM gamma-ray and proton induced insertion loss response data.

greater loss under equivalent dose proton irradiations compared to the gamma-ray responses. A single datum for IPITEK device MZ-100 irradiated by protons is shown which is highly elevated in loss compared to the losses observed for the SNDP proton-irradiated devices. This trend exhibited in both gamma-ray and proton irradiated IPITEK devices seems to be consistent, again suggesting less radiation resistance for the IPITEK devices compared to either PWI or SNDP devices. However, until additional response data is acquired from a sufficiently large sample size, and at higher dose, the understanding of the relative radiation resistance between PBMs differing in composition and processing methodologies will not be thoroughly understood.

Shown in Figure 33 are comparisons of the extinction ratio responses for SNDP and PWI paired PBMs following irradiation by protons and gamma-rays. The responses are mixed

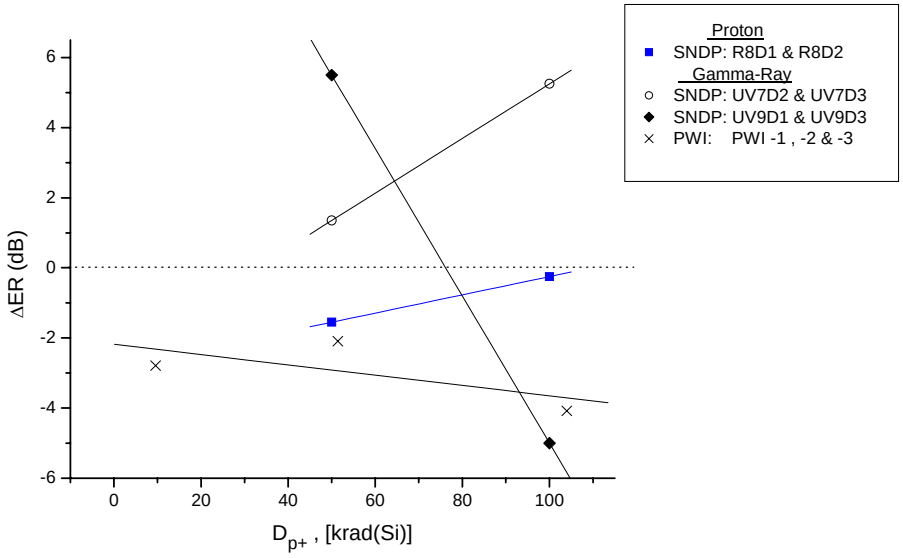

Figure 33. Fusion of PBM gamma-ray and proton induced ER response data.

for the gamma-ray and proton irradiated devices indicating ER instability among some of the devices. The proton irradiated paired SNDP devices exhibited an initial decrease in ER at low dose followed by an increase in ER at higher dose effectively restoring the ER to its pre-irradiation value. Of particular significance is that the ER response data shown for the proton irradiation of SNDP devices are considerably reduced in magnitude compared to the gamma-ray irradiated devices at the dose D_{γ} = 50 krad(Si), suggesting that the energetic protons may have induced greater degradation in the PBMs via dislocation effects rather than strictly ionization processes. The PWI data shows substantial and continued reduction in ER with increasing dose, indicating greater ER sensitivity to gamma-ray irradiation compared to the SNDP devices.

Interpretation of the of the contrasting results shown in Figure 33 remains an open issue since additional studies with a larger number of samples are required to ascertain the exact nature of the mixed ER responses. However, potential sources of error leading to the mixed results may include differing ER measurement systems among the participating device providers, and differences in their approaches used in performing passive pre- and post- irradiation measurements. Errors and error propagation can be

minimized by performing *in situ* ER measurements before, during and after the irradiation.

Shown in Figure 34 are fusions of all insertion loss data for gamma-ray irradiated paired and unpaired SNDP CLD-based devices and PWI paired devices.

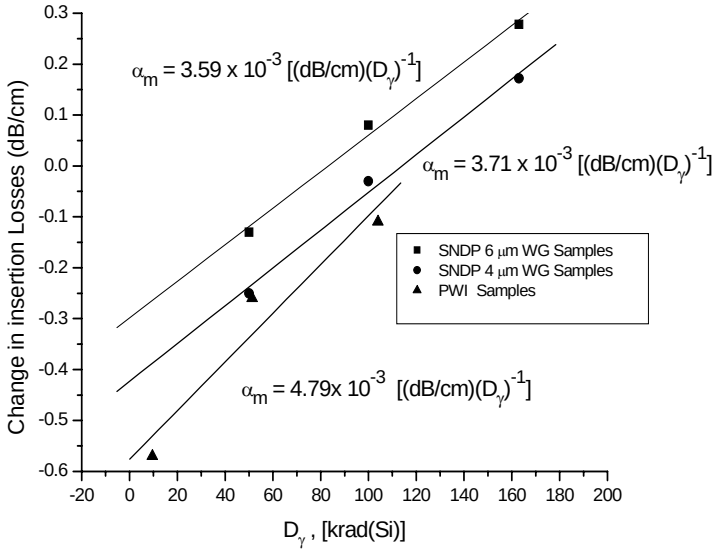

Figure 34. Fusion of IL gamma-ray irradiation data from SNDP Sample Sets 2 and 3. PWI device responses show a greater degradation rate.

PWI paired devices. The device loss data from Figure 15 was combined with the averaged loss data of Figure 16 allowing comparison of the loss responses to higher dose [D_γ = 163 krad(Si)]. By including the high dose loss data of SNDP Sample Set 3, the gamma-ray degradation rates in Figure 34 were reduced compared to the waveguide degradation rates derived at lower dose and previously shown in Figure 15. Reduction to the 4 and 6 μm degradation rates were 14.5% and 15.6 % relative to those shown in Figure 15. The degradation rates representing the SNDP 4 and 6 μm waveguide loss responses shown in Figure 34 agree within 3.28% or (within the uncertainty of the loss measurements). Figure 34 also compares the SNDP CPW-1/APC data to the PWI CLD-75/APC data, the latter exhibiting a higher degradation rate.

Figure 35 shows the paired PBM data of SNDP Sample Set 2 in Table 4 combined with the averaged response data of Sample set 3 (shown in Table 5) and fitted with a linear regression curve. As can be observed, there is good agreement in the curve-fitted degradation rates for SNDP and PWI sample responses [rates of -0.04067 %$(D_\gamma)^{-1}$ and -0.04354% $(D_\gamma)^{-1}$], respectively. Despite the large spread in the SNDP Sample set 2 and 3 data, the slope values of the PWI and SNDP data agree within 6.9%. These combined data clearly show that gamma-ray degradation to the half-wave voltages of SNDP and PWI devices decreased with increasing dose over the dose range applied. The large contrast in differing degradation rates and scatter in the data between SNDP Sample Set 1

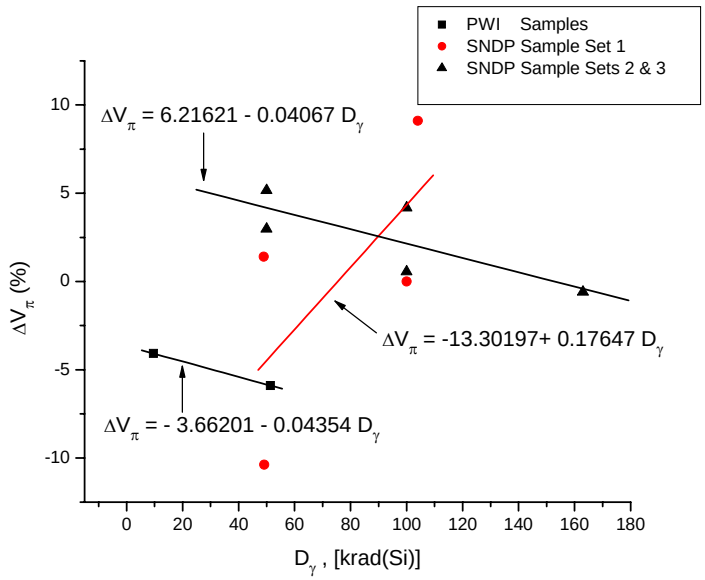

Figure 35. Fusion of ΔV_π gamma-ray irradiation data. The comparable linear regression curve fits for SNDP Sample Sets 2 and 3 and PWI data suggest that the conductance of the device samples is increasing and the half-wave voltages are decreasing as a result of the irradiation process. This response behavior is contrasted with much earlier SNDP (Sample Set 1) data. The differences in the SNDP data sets are believed in part due to Samples Sets 2 and 3 devices receiving stronger poling and experiencing improved measurement techniques.

and SNDP Samples 2 and 3 is very apparent. The differences are believed due to Sample Sets 2 and 3 undergoing stronger poling and improved pre- and post-irradiation measurements. An important issue raised by the SNDP and PWI response data is whether ΔV_π continues to decrease with increasing dose, saturates or perhaps begins to reverse

direction at higher dose. Recently conducted IPC experiments on a hybrid Poly S-119 PBM device a showed strong indication of ΔV_π beginning to saturate after receiving a mixed gamma-ray and proton total dose of 209 krad(Si) [22].

Additional high dose irradiations of the SNDP and PWI modulators would provide answers to this open and very interesting issue which could be accomplished using either *passive* or *in situ* irradiation approaches. If for example high dose irradiation resulted in saturation, an upper bound to the radiation resistance of PBMs would be established. Under this ideal situation, physical response models relating the device dependency on fabrication parameters such as materials processing, poling conditions, influence of unwanted impurity content, etc. could be formulated and experimentally investigated for verification. The end result would be the optimization of extremely radiation resistant modulators appropriate for space and strategic applications.

Finally, Figure 36 shows the collective data of SNDP sample sets 2-4 portrayed as 2 cm equivalent push-pull modulators. However, the correspondence in doing this comparison

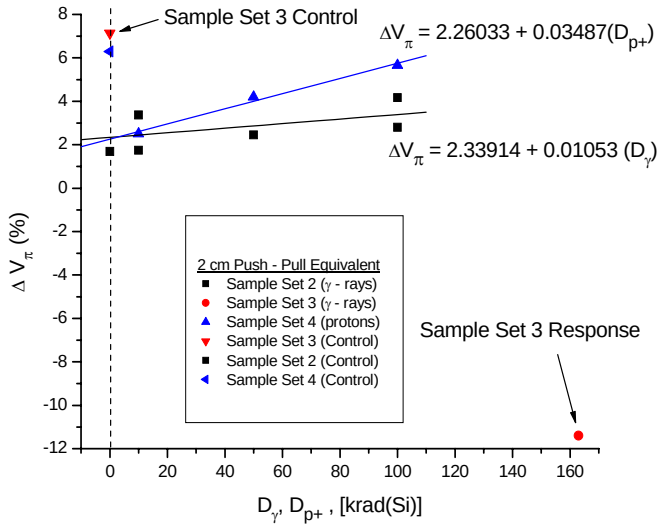

Figure 36. Representation of 2 cm equivalent push pull irradiation responses.

is not 1:1 since the SNDP samples were single-arm modulators having either 1 or 2 cm interaction lengths as discussed previously. As can be seen in Figure 36, the degradation

rate for the proton irradiated PBMs in Sample Set 4 exceeds the rate exhibited by the gamma-ray-irradiated devices in Sample Set 2. The average of the ΔV_π responses of Sample Set 3 irradiated at D_γ = 163 krad(Si) are shown as a single point (ΔV_π = -11.4 V). The non-irradiated control device for this data set also showed a dramatic increase in V_π indicating substantial aging response to environmental factors. Conversely the effects of aging appear to be significantly offset in the irradiated devices in Sample Set 3 irradiated at the highest dose [D_γ = 163 krad(Si)] indicating perhaps a beneficial interaction between the gamma-rays and known trapped oxygen in the CPW-1/APC polymer layers that can be been activated by light resulting in deterioration and destruction of the chromophores. These responses might indicate that to some extent trapped oxygen in the polymer layers which can lead to V_π reduction via chromophore deterioration were neutralized or released in the ionization process. Radiation caused increases to the device free volume may have promoted promoting permeability in the polycarbonate. Polycarbonate is known to undergo simultaneous cross-linking and scission with cross-linking predominating at low dose < 5 Mrad(Si) while scission predominates at higher dose [23]. Both processes can increase the free volume and reverse of physical aging as evidenced by “de-aging” reported for polystyrene, poly(methyl methacrylate) and poly carbonate irradiated by electrons [24].

CONCLUSIONS

Passive gamma-ray and proton irradiation of state-of-the–art and emerging polymer based modulators (PBMs) and NLO modulator materials provided by AFRL organizations and commercial sources were successfully investigated to determine their potential for eventual airborne and space environment microwave applications. PBMs with active core regions composed of CPW-1/APC, CLD-75/APC, LD3, PCBS and other electro-optic linear and non-linear materials were irradiated to ionizing doses ranging to ~ 163 krad(Si).

There were considerable variations in reported modulator pre- and post- radiation induced parameter response data between the different participating device providers and even within the individual sample sets of several of the providers. Factors such as differing measurement uncertainties, poling techniques, materials processing, device compositions, lack of information on impurity levels, etc. presented an interesting challenge for conducting a comparative analysis of the pre-and post irradiation data. However, in many instances the response data was observed to be consistent especially in devices composed of similar core and cladding materials. Data indicated that irradiation at low dose in some devices resulted in reductions to the insertion losses and half-wave voltages. These responses might indicate that to some extent annealing or ionization induced trap-filling of inherent defects occurred or perhaps trapped oxygen in the polymer layers which can lead to device instabilities via chromophore deterioration were neutralized or released in the ionization process via radiation induced increases to the device free volume promoting permeability. However, additional *passive* or *in situ* irradiation investigations would be required to confirm these desirable effects.

Changes in key modulator operational parameters including half-wave voltage, insertion losses and extinction ratios were evaluated following the irradiation by gamma-rays and protons. Among the different spun-on and self-assembled PBMs studied, CLD-1 (i.e. CPW-1) devices exhibited the greatest resistance to both gamma-rays and proton irradiations. However, considerable anomalies in the response data were observed

indicating the need for performing *in-situ* studies for resolution. A summation of the effects of ionization induced effects key parameter results are as follows:

Half-wave voltage responses

Empirical data in support of a recent hypothesis asserting that strongly poled PBMs exhibiting low half-wave voltages are less susceptible to moderate gamma-ray dose was demonstrated by SNDP and PWI PBMs. Half-wave voltages in PWI- PBMs and SNDP-paired PBM samples were observed to decrease with increasing dose. The gamma-ray-induced changes in V_π observed for the PWI CLD-75/APC devices was similar to the SNDP APC/CPW-1 device responses as evidenced by the close agreement in their fitted linear regression response curves and degradation rates. Gamma-ray irradiated PWI devices exhibited slightly suppressed V_π responses relative to SNDP devices and both SNDP and PWI devices exhibited a high potential for withstanding gamma-ray irradiation at higher dose. Since the driving voltages in SNDP paired devices and devices within the PWI sample set appear to consistently decrease with increasing dose this suggests that the conductance of the polymer based devices gradually increased with increasing dose. The increased degradation rate observed for the proton irradiations at equivalent dose was attributed to dislocation as well as ionization induced effects within the core and cladding regions of the modulator. The decrease in V_π values following the gamma-irradiated devices at low dose are believed due to an increase in free volume predominantly resulting from the interaction of gamma-rays with the core materials and initially causing cross-linking and scission to improve the device conductivity. The CPW-1/APC devices also show that the eventual reduction in V_π lies well beyond the 163 krad(Si) irradiation data.

V_π degradation rates for SNDP paired modulators (Sample Sets 2 and 3) and the PWI sample set both composed of CLD core materials agreed within 6.9%. However, confidence in this response behavior is limited to the total dose range of ~ 10-163 krad(Si) and may not be valid at much higher dose and raises an important issue whether ΔV_π continues to decrease with increasing dose, saturates or perhaps begins to reverse direction at significantly higher dose.

Recently conducted IPC experiments on a hybrid Poly S-119 PBM showed strong indications of ΔV_π beginning to saturate after receiving a mixed gamma-ray and proton total dose of 209 krad(Si). If high dose irradiation resulted in saturation, an upper bound to the radiation resistance of CPW-1/APC -based PBMs would be established. Under this ideal situation, physical response models relating the device dependency on fabrication parameters such as materials processing, poling conditions, influence of unwanted impurity content, etc. could be formulated and experimentally investigated for verification. The end result would be the optimization of extremely radiation resistant CPW-1/APC modulators appropriate for space and strategic applications.

There were significant variations between the devices in regards to their individual core and cladding materials, thickness, electrodes and poling conditions. Regardless, devices based on CPW-1/APC and CLD-75/APC devices both having low V_π values showed the highest radiation resistance compared to the other devices investigated. Proton irradiations of PBMs at equivalent dose may have induced greater degradation in SNDP PBMs via dislocation effects rather than strictly ionization processes. The degradation rate of the half-wave voltage was observed to increase from an average of -3.41×10^{-2} [% $(D_\gamma)^{-1}$] for gamma-ray irradiated SNDP samples to 8.31×10^{-2} [%$(D_{p+})^{-1}$] under proton irradiation.

Insertion loss responses

The insertion loss response data of paired and irradiated SNDP 4 and 6 μm width straight waveguide samples were minimally affected by either gamma-rays or protons over the dose range applied and as a result of the gamma-ray irradiations, the losses were slightly suppressed. Following low dose gamma-ray irradiations, an initial decrease in SNDP, PWI and IPITEK device insertion losses were first observed next followed by increasing loss for increasing dose. The average long-term gamma-ray induced degradation rate for the propagation loss of all samples within SNDP Sample set 2 was $\alpha_m = \sim 9 \times 10^{-4}$ [dB·cm^{-1} $(D_\gamma)^{-1}$] and $\sim 4.3 \times 10^{-3}$ [dB·cm^{-1} $(D_\gamma)^{-1}$] within paired devices indicating good

waveguide uniformity among the different chips. The corresponding loss in PWI PBMs was determined to be $\alpha_m = 4.8 \times 10^{-3}$ [dB·cm^{-1} $(D_\gamma)^{-1}$] while the change in loss exhibited by IPITEK devices was approximately an order of magnitude higher at $\alpha_m = 4.79 \times 10^{-2}$ [dB·cm^{-1} $(D_\gamma)^{-1}$]. Losses from proton irradiations of SNDP PBMs ranged from 0.05-0.23 dB·cm^{-1} [0-100 krad(Si)] compared to the proton-irradiated IPITEK device's change in insertion loss of 1.0 dB·cm^{-1} at a total dose of 100 krad(Si). The SNDP PBM paired samples consisting of 4 and 6 μm waveguides exhibited post-irradiation changes to losses within ~ 0.18 dB·cm^{-1} over the dose range 10-100 krad(Si). Substantial aging was noted for the non-irradiated Control devices since loss data exhibited by several Control devices exceeded the average loss in the SNDP proton irradiated samples. The data revealed that the average initial loss of SNDP PBMs at 50 krad(Si) was greater for proton irradiation than for equivalent gamma-ray dose, exhibiting a loss of ~0.19 and 0.08 dB·cm^{-1} at 50 and 100 krad(Si), respectively.

Extinction ratio responses

While ER responses were mixed for SNDP paired devices it was observed that following proton irradiations, the ER initially decreased at a dose of 50 krad(Si) and next significantly increased at 100 krad. This behavior contrasted with other gamma-ray irradiated SNDP paired devices and the PWI device responses. The gamma-ray irradiated PWI devices exhibited considerable reduction in ER at a dose of ~50 krad(Si) with ER observed increasing for increasing dose.

External, environmental and aging factors

The post-irradiation ER responses of various *non-irradiated* Control samples often showed as much variation in parameters as the irradiated samples, suggesting the presence of photo-induced instabilities within the devices. The scatter in all sample pre- and post-irradiation response data may have also occurred due to the measurement uncertainty or differences in interpretation of measurement data among the device contributors. Since the EO chromophores used in the CLD-1-based devices were known to be light-sensitive, photo-induced chemical changes were believed to have occurred

during the brief period that the devices were exposed to light, a necessary condition for performing pre-and post-irradiation characterization. Trapped oxygen within the polymer layers may have been photo-activated resulting in the deterioration and destruction of the chromophores. Most likely all these processes were present to some extent causing relaxation of the device poling. The presence of high propagation and insertion losses in some devices also supports the contention that defects (causing light absorption) and optical scattering centers as well as impurities introduced within the device during the fabrication process were affected by the ionization process.

The empirical data resulting from the investigation provides a first but critical step in addressing DOD concerns for determining the potential suitability of polymer-based photonic technologies for aerospace and space microwave system applications. Of particular interest is the steady improvement noted in the SNDP CPW-1/APC irradiation response data with each successive generation of samples. Correlation with the PWI CLD-75/APC samples indicates that improved SNDP polymer modulators free of unwanted impurities and precursors that interact deleteriously with ionizing radiation will result in highly radiation resistant devices for space and strategic system applications.

RECOMMENDATIONS

Conduct additional *passive* gamma-ray and proton irradiation investigations of emerging polymer modulators and materials. This will significantly increase the AFRL/SNDP irradiated PBM database advancing the development of mathematical response models describing the interaction and response of the polymer based device parameters to specific material parameters and processing. This approach is relatively inexpensive and allows simultaneous irradiation of a large number of devices to high doses in a reasonable time period. Passive irradiations reveal long-lived residual changes (i.e. degradation) of the component parameters which are directly attributable to the irradiation process. Passive studies are important for assisting AFRL/SNDP in selecting viable PBM materials, designs and processing protocols early in the modulator development assuring radiation resistant technology. Immediate goals for improving future passive studies include:

- *Increase number of device in samples sets to improve data statistics.*
- *Irradiate samples incrementally over the range to doses of 10-1000 krad(Si).*

Conduct *in situ* gamma-ray and proton irradiation investigations of key emerging polymer modulators and materials. Irradiation of discreet components under *in situ* conditions provides an enormous amount of time-and dose resolved data regarding the devices' responses prior to, during and after irradiation. By controlling the extent of radiation-induced degradation, catastrophic failure of the sample at high dose can be quickly adverted and a precise study of the kinetics involving the recovery from the degradation processes can be initiated. Precise measurement and acquisition of key modulator parameter data can be accomplished before, during and after irradiation, thereby limiting the inaccuracies often incurred in performing passive irradiations. Since the polymer sample is firmly set in place (*in situ*) at the irradiation source and operating before, during and after the irradiation process, removal of the sample from the irradiation source is not necessary to perform parameter measurements at off-site

locations as is typically encountered in *passive* irradiations. This minimizes error sources and assures repeatability in the *in situ* measured data.

- *In situ irradiations of operational components using protons (and/or electrons) with varying energies are necessary in order to examine the potential dislocation effects that result from the interaction of energetic particles with different polymer devices*. In inorganic crystal–lattice structured materials, energetic particle-induced dislocations of lattice atoms are much more deleterious to materials and device operation than are strictly ionization induced effects produced by gamma-rays. Dislocation effects usually result in permanent damage, whereas most of the deleterious effects reported for EO polymers irradiated by gamma-rays are somewhat recoverable in time via photo-induced or temperature annealing processes.

- *Device responses can be continuously observed during in situ irradiations and parameters can be manipulated under operational conditions.* This allows dynamic stressing and manipulation of the modulator key operational parameters as well as the ability to determine if photo-bleaching or trap-filling of induced or inherent defects is occurring. Dynamic measurements are not possible with *passive irradiations*. By being able to constantly observe and record the temporal responses of the modulators during the *in situ* irradiations, it should be possible to gain an understanding and verify recent AFRL/SNDP data with other DOD data indicating that degradation of NLO parameters in certain polymers saturate at moderate dose, thus indicating a high potential for developing a radiation resistant polymer device [9-11, 22].
- *In situ irradiations allow the rapid study of device/material recovery kinetics.* Observation and measurement of peak damage induced in polymer modulators and the subsequent early time dependent recovery kinetics are not possible with *passive* irradiations. Knowledge of the *peak* damage experienced by NLO polymers during the irradiation is important for developing mathematical models to predict the time required for a device to recover from degradation. *In situ*

studies allow the development of accurate models to explain nuances arising from potential degradation to charge carrier processes, material conductivity, and, to understand the particular influence of color centers and traps resulting from the irradiation process.

IPC recommends that gamma-ray and proton *in situ irradiations* be conducted as soon as possible to identify the most radiation resistant polymer materials and modulator devices for hardened and survivable microwave technology for space applications. Identification of radiation resistant NLO polymer technology in the early stages of modulator development will provide considerable cost savings in avoiding last-minute development programs to harden a 'soft" technology. Choice of radiation resistant materials early in the development cycle will also result in an early deployment of a well-developed radiation resistant EO polymer modulator.

REFERENCES

[1] E. W. Taylor, J. Nichter, F. Nash, R. Michalak, F. Haas, P. Payson, P. Cook, T. McEwen, B. McKeon, A. Szep, B. Flushe, A. Pirich, G. Brost, J. Grote, J. Zetts, P. Yaney, E. Heckman**,** "Behavior of NLO Polymer Modulators Irradiated by Gamma- Rays" *Proc. SPIE*, **5212**, 6 August 2003.

[2] E. W. Taylor, "Measurement of Radiation Induced Effects in Nonlinear Optic Modulators", *Proc. 49th ISA/IIS*, Orlando, FL, 4-8 May 2003.

[3] J. Grote, J. S. Zetts, R. L. Nelson, D. E. Diggs, F. K. Hopkins, P. P. Yanley, C. Zhang, W. H. Steier, M. C. Oh, H. R. Fetterman, A. K.-Y. Jen, L. R. Dalton, E. W. Taylor, J. E. Winter, A. D. Sanchez, D. M. Craig, "Nonlinear Optic Polymer Electro-Optic Modulators for Space Applications", *Proc. SPIE*, **4823**, *Photonics for Space Environments Conference VIII*, Seattle, WA, July, 2002.

[4] E. W. Taylor, R. Claus, K. Cooper, L. R. Taylor**,** "Gamma-Ray Irradiation and Responses of Electrostatically Assembled Electro Optic Polymer Materials**"**, *EOS/SPIE Symposium on Remote Sensing, Proc. SPIE,* **4547**, *Photonics for Space and Radiation Environments II Conference*, Toulouse, France, 17-21 Sept. 2001.

[5] E. W. Taylor, "Inorganic and Polymer Photonic Sensor Technologies in Space Missions", *Proc. 18th IEEE Instrumentation and Measurement Conference*, Budapest, Hungary, 21-23 May 2001.

[6] E. W. Taylor, A. Pirich, L. R. Taylor, "Qualifying Photonics for Space Environments*" Proc. 47th ISA International Instrumentation Symposium*, Denver Colorado, May 2001.

[7] E. W. Taylor, J. Grote, J. Zetts, J.E. Winter , A. D. Sanchez , D. Craig, "In Situ High Energy Proton Irradiation of Nonlinear Organic Modulator Materials for Space Environments", *Proc. SPIE,* **4134**, *Photonics for Space Environments Conference VII*, San Diego, CA, 1 August, 2000.

[8] J. G. Grote, E. W. Taylor, J. S. Zetts, J. E. Winter, A. D. Sanchez, D. Craig, F. K. Hopkins, "Optical Transmission and Thermal Heating Effects Due to Irradiation of Nonlinear Optic and Conductive Polymers for Space Based Electrooptic Applications", *Proc. SPIE*, **4134**, *Photonics For Space Environments VII*, 31 July- 1 August, 2000.

[9] E. W. Taylor, D. Le, M. F. Durstock, B. E. Taylor, R. O. Claus, T. Zeng, C. P. Morath, D. Cardimona, "Space Radiation Induced Effects in Polymer Photo-Detectors", *Proc. SPIE*, **4128,** *Photonics for Space Environments Conference VIII,* Seattle, WA, July, 2002.

[10] E. W. Taylor, T. Zeng, R. O. Claus, Advancement of Polymer Detectors for Space Applications, (Technical Report *AFRL-VS-PS-TE-2004-1049*, 16 March 2004) under AFRL review.

[11] E. W. Taylor, Investigation of Radiation Resistant Polymer Photodetectors for Space Applications**,** *AFRL-VS-TR-2002-1105*, Air Force Research Laboratory, Space Vehicles Directorate, Kirtland AFB, NM, 11 September 2002.

[12] E. W. Taylor, "Radiation Effects", Chapter 14.1 in: Properties of Lithium Niobate and Other Novel Ferroelectric Materials, Editor, K.K. Wong, *INSPEC Pub., IEE EMIS Datareview Series* No. 28, UK, July 2002.

[13] M.-C.Oh, H. Zhang, C. Zhang, H. Erlig, Y. Chang, B. Tsap, D. Chang, A. Szep, W. H. Steier, H. R. Fetterman, L. R. Dalton, "Recent Advances in Electroopric Polymer Modulators Incorporating Highly Nonlinear Chromophore*", IEEE J. Selected Topics in Quantum Electronics,* **7**, No.5, p. 826, September/October 2001.

[14] C. Zhang, L. R. Dalton, M. C. Oh, H. Zhang, W. H. Steirer, "Low V_π Electrooptic Modulators from CLD-1: Chromophore Design and Synthesis", Material Processing and Characterization", *Chem. Mater*, Vol. 13, 2001.

[15] "Standard Practice for Minimizing Dosimetry Errors in Radiation Hardness Testing of Silicon Devices Using Co-60 Sources", ASTM Committee E10.07 on Nuclear Technology and Applications, Designation: E 1249-00, July, 2000.

[16] J. C. Salamone, Concise Polymeric Materials Encyclopedia, CRC Press, 1999.

[17] M. D. Barkley, B. H. Zimm, *J. Chem. Phys*., **70,** 1979.

[18] M. Wanatabe et. al., *Int. J. Radiat. Biol*., **61**, 1992.

[19] K. Takakura et. al., Synchrotron Radiation in Biosciences, Clarenden, Oxford, UK, 1994.

[20] K. Heida, T. Ito, Handbook on Synchrotron Radiation, Elsevier Science, Amsterdam, 1991.

[21] J. F. Zigler, j. P. Biersack, U. Littmark, The Stopping and Ion Range of Ions in Matter, Pergamon, New York, 1985.

[22] E. W. Taylor, D. Wood, R. O. Claus, Polymer Based Photonics for Space Environment Applications, (Technical Report *AFRL–VS-PS-TR-2004-1105*, 1 May 2004) under AFRL review.

[23] D. Acierno, F. LaMantia, G. Titomanlio, *Radiation Phys. Chem*., **16**, 95, 1980.

[24] D. C. McHerron, G. L. Wilkes, *Polymers*, **34**, No.5, 915, 1993.

APPENDIX A.1 POLING PROFILES

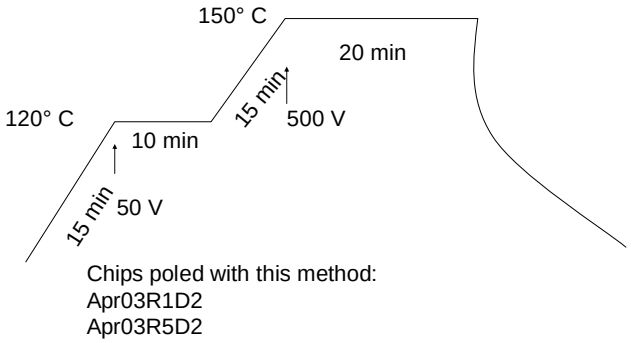

Figure A-1. PP-5 poling profile.

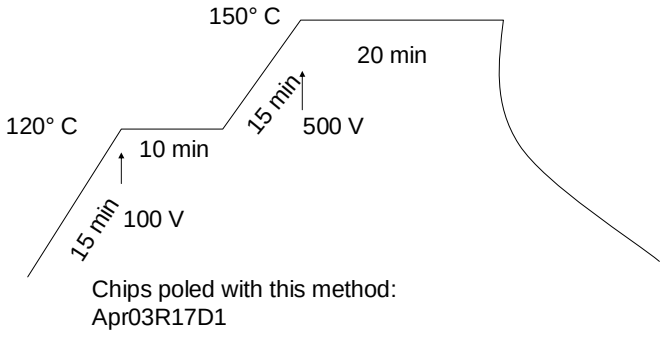

Figure A-2. PP-6 poling profile.

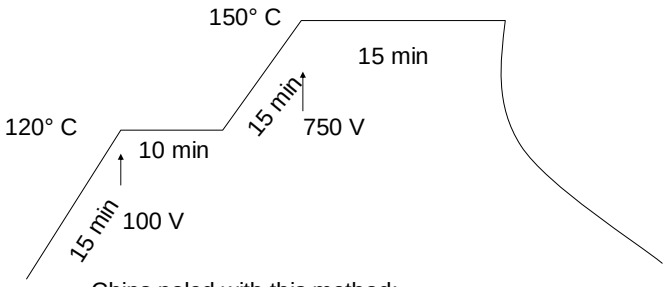

Figure A-3. PP-7 poling profile.

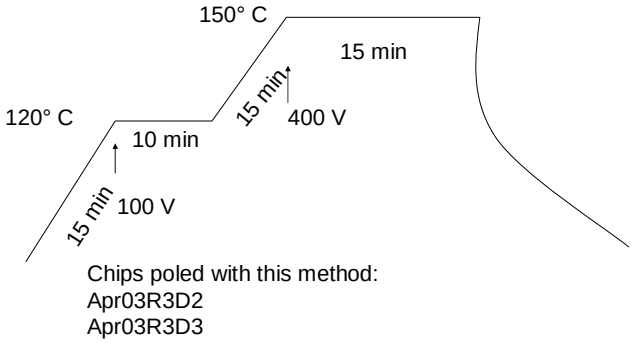

Figure A-4. PP- 8 poling profile.

APPENDIX A.2 IPITEK MEASUREMENT SETUP

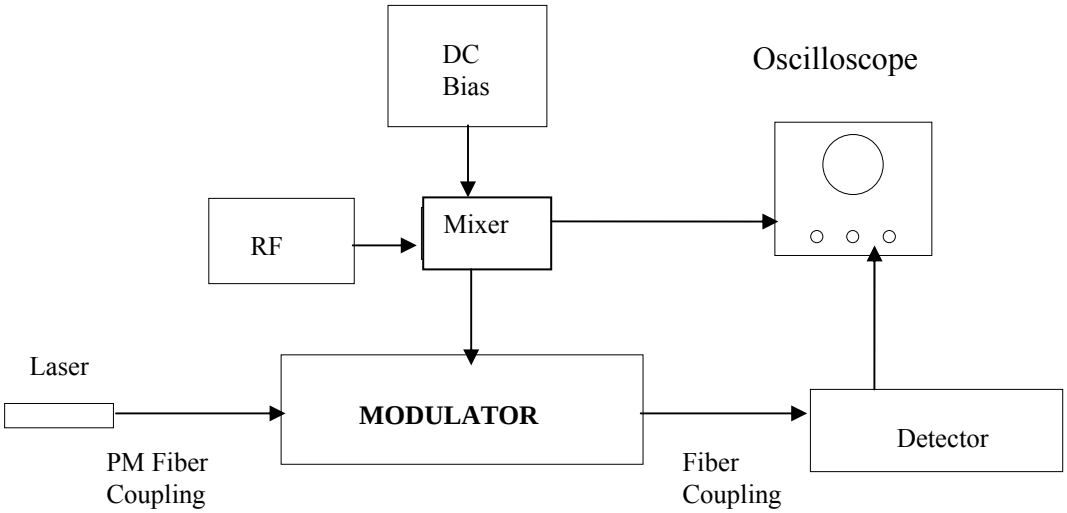

Figure A-5. IPITEK V_π measurement set-up.

APPENDIX A.3 PROTON DOSIMETRY

Table A.1. Proton Dosimetry for Irradiation of SNDP Sample Set 4.

Beam Type:	Proton	**FC/SEM Ratio:**	1.145 ± 1.006E-3		**File Name:**				
Beam E (MeV):	25.6	**FC Lkg (A):**	-2.14E-13 ± 1.74E-13		m:\Ref_user\InternationalPhotonics\ITPhotonics_November24_(				
Target:	Si	**SEM Lkg (A):**	1.19E-12 ± 1.588E-12						
dE/dx(MeV/(g/cm²):	16.826								
Date: 11/24/03									
	Run Time (s)	**Mean Current (A)**	**Std Dev <I> (A)**	**Incr Dose (rad)**	**Acc Dose (rad)**	**Incr Fluence (p/cm²)**	**Acc Fluence (p/cm²)**	**Avg Dose Rate (rad/s)**	**Beam Profile**
Run # 1									
9:22:26 AM	24.062	9.21E-09	1.698E-11	1.02E+04	1.02E+04	3.77E+10	3.77E+10	4.23E+02	0 - 0.5 cm
Box # 3 AFRL/SNDP				1.01E+04	1.01E+04	3.76E+10	3.76E+10	4.21E+02	0.5 - 1.5 cm
				9.95E+03	9.95E+03	3.69E+10	3.69E+10	4.14E+02	1.5 - 2.5 cm
Run # 2									
9:29:07 AM	110.069	9.92E-09	3.425E-13	5.01E+04	5.01E+04	1.86E+11	1.86E+11	4.56E+02	0 - 0.5 cm
Box # 1 AFRL/SNDP				5.00E+04	5.00E+04	1.85E+11	1.85E+11	4.54E+02	0.5 - 1.5 cm
				4.90E+04	4.90E+04	1.82E+11	1.82E+11	4.46E+02	1.5 - 2.5 cm
Run # 3									
9:33:45 AM	109.68	9.95E-09	6.138E-13	5.02E+04	5.02E+04	1.86E+11	1.86E+11	4.57E+02	0 - 0.5 cm
Box # 4 AFRL/SNDP				5.00E+04	5.00E+04	1.85E+11	1.85E+11	4.56E+02	0.5 - 1.5 cm
				4.90E+04	4.90E+04	1.82E+11	1.82E+11	4.47E+02	1.5 - 2.5 cm
Run # 4									
9:39:58 AM	219.97	9.91E-09	8.134E-13	1.00E+05	1.00E+05	3.71E+11	3.71E+11	4.55E+02	0 - 0.5 cm
Box # 2 AFRL/SNDP				9.97E+04	9.97E+04	3.70E+11	3.70E+11	4.53E+02	0.5 - 1.5 cm
				9.79E+04	9.79E+04	3.63E+11	3.63E+11	4.45E+02	1.5 - 2.5 cm
Run # 5									
9:46:58 AM	221.402	9.83E-09	5.572E-13	1.00E+05	1.00E+05	3.71E+11	3.71E+11	4.52E+02	0 - 0.5 cm
Box # 5 AFRL/SNDP				9.96E+04	9.96E+04	3.70E+11	3.70E+11	4.50E+02	0.5 - 1.5 cm
				9.78E+04	9.78E+04	3.63E+11	3.63E+11	4.42E+02	1.5 - 2.5 cm
Run # 6									
9:54:14 AM	217.501	1.00E-08	2.185E-13	1.00E+05	1.00E+05	3.71E+11	3.71E+11	4.60E+02	0 - 0.5 cm
Box # 6 AFRL/SNDP				9.98E+04	9.98E+04	3.70E+11	3.70E+11	4.59E+02	0.5 - 1.5 cm
				9.79E+04	9.79E+04	3.63E+11	3.63E+11	4.50E+02	1.5 - 2.5 cm
Run # 7									
10:00:58 AM	219.099	9.95E-09	4.753E-14	1.00E+05	1.00E+05	3.71E+11	3.71E+11	4.57E+02	0 - 0.5 cm
Box # 7 AFRL/SNDP				9.98E+04	9.98E+04	3.70E+11	3.70E+11	4.55E+02	0.5 - 1.5 cm
				9.79E+04	9.79E+04	3.63E+11	3.63E+11	4.47E+02	1.5 - 2.5 cm
Run # 8									
10:07:55 AM	220.961	9.87E-09	1.016E-14	1.00E+05	1.00E+05	3.71E+11	3.71E+11	4.53E+02	0 - 0.5 cm
Box # 8 AFRL/SNDP				9.98E+04	9.98E+04	3.70E+11	3.70E+11	4.52E+02	0.5 - 1.5 cm
				9.79E+04	9.79E+04	3.63E+11	3.63E+11	4.43E+02	1.5 - 2.5 cm